AD-775 577

HIGH POWER DYE LASERS

A. R. Clobes, et al

United Aircraft Research Laboratories

Prepared for:

Office of Naval Research
Advanced Research Projects Agency

28 February 1974

SECURITY CLASSIFICATION OF THIS PAGE (When Data Entered)

REPORT DOCUMENTATION PAGE

READ INSTRUCTIONS BEFORE COMPLETING FORM

1. REPORT NUMBER: N921617-5	2. GOVT ACCESSION NO.
3. RECIPIENT'S CATALOG NUMBER: AD775 577	
4. TITLE (and Subtitle): HIGH POWER DYE LASERS	5. TYPE OF REPORT & PERIOD COVERED: Annual Technical 1/1/73 - 2/28/74
	6. PERFORMING ORG. REPORT NUMBER: N 921617-5
7. AUTHOR(s): Clobes, A. R., Ferrar, C. M., Glenn W. H., Ladd, G. L., Morey W. W.	8. CONTRACT OR GRANT NUMBER(s): N00014-73-C-0284
9. PERFORMING ORGANIZATION NAME AND ADDRESS: United Aircraft Research Laboratories, 400 Main Street, E. Hartford, Conn 06108	10. PROGRAM ELEMENT, PROJECT, TASK AREA & WORK UNIT NUMBERS: ARPA
11. CONTROLLING OFFICE NAME AND ADDRESS: Office of Naval Research, Department of Navy, Arlington, VA 22217	12. REPORT DATE: 2/28/74
	13. NUMBER OF PAGES: 75
14. MONITORING AGENCY NAME & ADDRESS (if different from Controlling Office): Director, Physics Programs, Physical Sciences Division, Office of Naval Research, 800 N Quincy Street, Arlington VA 22217	15. SECURITY CLASS. (of this report): Unclassified
	15a. DECLASSIFICATION/DOWNGRADING SCHEDULE

16. DISTRIBUTION STATEMENT (of this Report)

Approved for public release, distribution unlimited

17. DISTRIBUTION STATEMENT (of the abstract entered in Block 20, if different from Report)

18. SUPPLEMENTARY NOTES

19. KEY WORDS (Continue on reverse side if necessary and identify by block number)

High Power Dye Lasers
Flashlamps
Frequency Sweeping

20. ABSTRACT (Continue on reverse side if necessary and identify by block number)

This report describes the operation of a high power, repetitively pulsed, flashlamp pumped dye laser. To date an average power of 39 watts at a repetition rate of 100 Hz has been obtained. The techniques employed should be scalable to higher power and higher repetition rate. Experiments to produce frequency sweeping of the laser during the pulse are described. Altimate flashlamp geometries are discussed as are experiments to achieve better spectral matching of the lamp output to the dye.

DD FORM 1 JAN 73 1473 EDITION OF 1 NOV 65 IS OBSOLETE,

SECURITY CLASSIFICATION OF THIS PAGE (When Data Entered)

UNITED AIRCRAFT CORPORATION
RESEARCH LABORATORIES

Report Number: N-921617-5
Semi-Annual Technical Report for the period
1 January 1973 to 28 February 1974

HIGH POWER DYE LASERS

ARPA Order No.	1806 AMEND #9/11-15-72
Program Code:	3E90
Contractor:	United Aircraft Research Laboratories
Effective Date of Contract:	1 January 1973
Contract Expiration Date:	28 February 1974
Amount of Contract:	$149,638.00
Contract Number:	N00014-73-C-0284
Principal Investigator	Dr. William H. Glenn (203) 565-5411
Scientific Officer:	Director, Physics Programs ONR
Short Title:	High Power Dye Lasers
Reported By:	A. R. Clobes, C. M. Ferrar, W. H. Glenn G. O. Ladd, Jr. and W. W. Morey

Sponsored By
Advanced Research Projects Agency
ARPA Order No. 1806

UNITED AIRCRAFT RESEARCH LABORATORIES

ANNUAL REPORT N-921617-5

TABLE OF CONTENTS

UNITED AIRCRAFT RESEARCH LABORATORIES

ANNUAL REPORT N-921617-5

TABLE OF CONTENTS

TABLE OF CONTENTS (Con't)

TECHNICAL REPORT SUMMARY

Under this contract, a high power, flashlamp pumped dye laser has been constructed and tested. To date the laser has produced an average power of 39 watts at a repetition rate of 100 Hz. The technique used to achieve this power level appears to be scalable to higher average power and to higher repetition rates (several thousand Hz). Section I of this report describes the operation of the laser at high power and high rates. The details of the construction of the laser have been described in the previous semi-annual technical report UARL N921617-2.

Section II of this report describes experiments to produce rapid frequency tuning of a dye laser during the laser pulse. A resonantly driven PZT transducer was used to modulate the transmission of a Fabry-Perot etalon. It was found possible to scan the output over a range greater than 100 A during the laser pulse. At present the instantaneous linewidth is approximately 20 A although it is expected that this could be reduced to about 1 A. This would provide 100 resolution elements within the pulse, or an effective 10 nsec resolution for a 1 microsecond pulse.

Section III discusses alternate geometries for the flashlamp which should allow operation at higher energies. The present lamp will withstand energies up to about 300 joules on a single shot basis, although catastrophic failure sometimes occurs at lower energy and high rates. Experiments were carried out on a geometry which completely eliminated the quartz envelope and established a vortex flow in the entire lower half of the pumping cavity. Stabilization at low rates appears to require a vortex flow somewhat larger than with a quartz envelope. Experiments have indicated, however, that the discharge may stabilize itself at sufficiently high rates (150 Hz).

Section IV of this report describes spectral measurements that have been made on a test arc discharge. These are part of a continuing effort to determine the optimum operating conditions of the lamp to maximize the efficiency for dye pumping.

Section V describes a related effect involving passive filtering to optimize the spectral matching between the flashlamp and the dye absorption characteristics.

An article entitled "Vortex Stabilized Flashlamps for Dye Laser Pumping" by M. E. Mack has been published in Applied Optics 13 46 (1974). This work was supported in part by the present contract.

SECTION I

HIGH POWER, HIGH REPETITION RATE DYE LASER OPERATION

1.1 Flashlamp Tests

As has been previously reported, earlier attempts to operate at high pulse repetition rates were limited by self-firing of the flashlamp at rather low voltages, whenever the pulse rate exceeded 20 or 30 pps. In order to overcome this problem we have added a spark gap in series with the flashlamp, such that the series gap provides the voltage holdoff required to prevent low voltage self-firing.* Rapid recovery of the series gap is assisted by gas flow across the gap and by a relatively small electrode spacing in this gap. The gap employed was initially assembled only for preliminary tests, with little attention paid to minimizing inductance and gap losses. However, the success of initial tests led to installation of the gap on the high power dye laser for further testing, in spite of these design short comings.

The waveform of the flashlamp light output with the series gap installed is shown in Fig. I-1 for a single shot at 140 joule lamp input energy. The shape of this waveform is very similar to that observed without the series gap, but the time scale is slower by 20 to 30 percent due to the inductance of the gap assembly (even though a previously used series inductor has been eliminated for these tests). The increased risetime, as well as any energy dissipation in the gap, can be expected to reduce the dye laser output. However, tests of the laser both with and without the series gap have shown that such reduction of laser output energy does not exceed 10 to 12 percent, even with the present crude gap design.

The effectiveness of the series gap is demonstrated in Fig. I-2, where repetitive flashlamp output pulses are shown at 20 pps and 100 pps, for lamp inputs of 106 joules per pulse. It may be noted that the pulse risetime is slightly shorter and the peak lamp output slightly higher at 100 pps than at 20 pps. Thus these important laser pumping characteristics of the lamp appear not to degrade, but in fact to improve slightly at the higher repetition rate, in spite of the fact that per-pulse lamp input energy tends to fall somewhat at high rates due to power supply limitations. The reason for this improvement is not yet clear but may be associated with pressure buildup in the lamp at high pulse rates. The observation of occasional abnormally intense pulses during lamp startup (seen faintly in Fig. I-2b) may also result from transient pressure phenomena. These anomalies are observed frequently at pulse rates of order 100 pps, but seldom at 20 pps or less, where pressure effects should be substantially smaller. It is not presently known whether these effects are directly related to an observed preponderance of catastrophic lamp failures

*The details of this specially designed gap will be given in a subsequent report.

FIG. I-1

SINGLE SHOT FLASHLAMP OUTPUT – – 140 JOULE INPUT

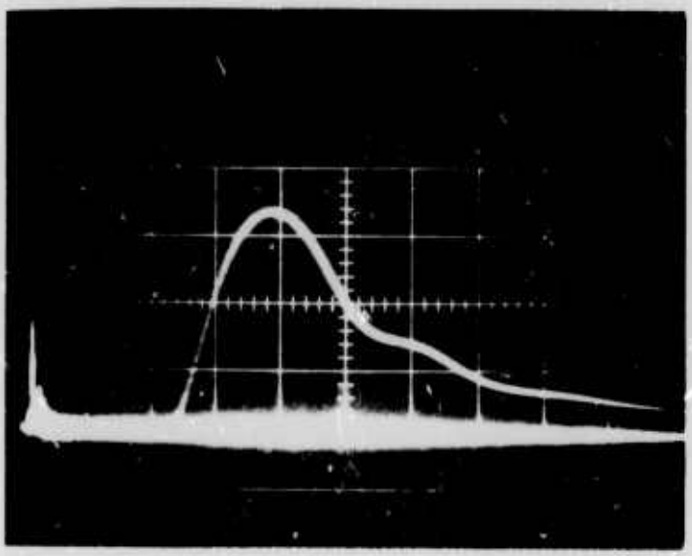

1.0 μsec/div ⟶

NO. 144

FIG. I-2

REPETITIVE FLASHLAMP OUTPUT – – 200 JOULE INPUT

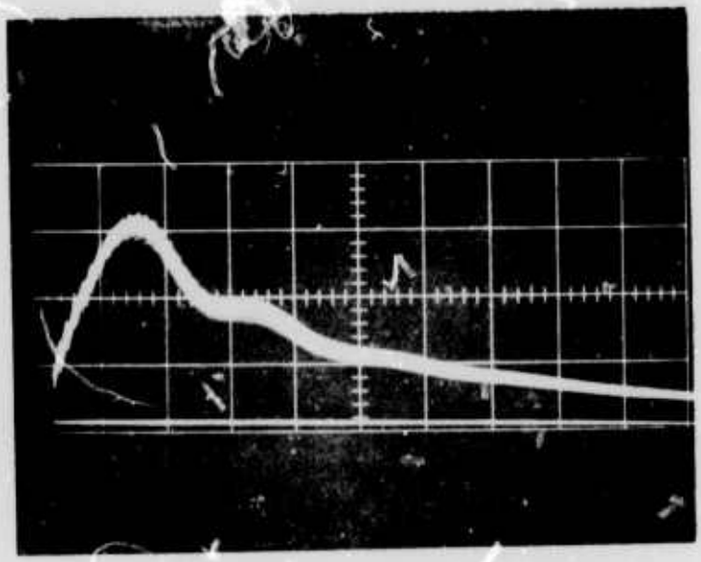

a) 20 pps
1.0 μsec/div

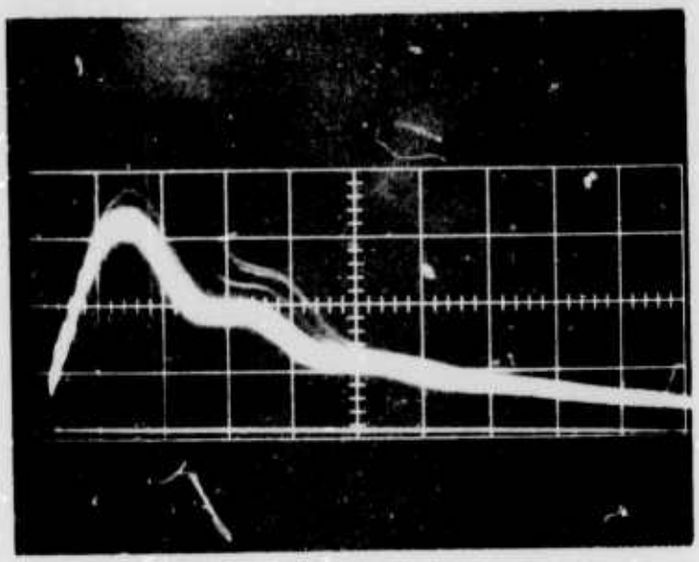

b) 100 pps
1.0 μsec/div

immediately following startup at high repetition rates. In any event, once the startup transients have subsided, regular, reproducible lamp output pulses have been obtained at rates at least up to 110 pps at 200 joules per pulse, and to 150 pps at 160 joules per pulse (i.e. 22 to 24 kw lamp input), being limited apparently only by power supply charging capabilities. Lamp self-firing appears to have been completely eliminated by the series gap, even at these high energies and repetition rates.

1.2 Laser Tests

The high power dye laser has been described fully in earlier reports. For the present tests, a series spark gap was added, as described in the preceding section, to allow high repetition rate flashlamp operation at high input energies. A 1.5×10^{-4} molar solution of Rhodamine 6G tetrafluoroborate in etnanol was filtered and pumped through the 8 mm i.d. by 75 mm long active dye cell volume at various controlled rates up to 0.63 liters per second. In these tests the laser power supply was set for a fixed nominal output voltage of 14 kv. This supply charged a 2 mfd capacitor which was then periodically discharged into the flashlamp via the series spark gap. Although no external charging resistance was used, the internal impedance (non-linear) of the power supply caused some reduction of the charging voltage at high pulse rates. For example, although the lamp input energy remained nearly constant at about 196 joules per pulse up to 80 pps, it dropped by about 5% at 100 pps and by an estimated 30% at 150 pps. The drop could be compensated by increasing the supply voltage setting, but this was not done for the tests reported in this section. Output power was extracted from the laser through a 42% transmitting dielectric-coated mirror and was measured using a Coherent Radiation Laboratories Model 201 Laser Power Meter. Extraneous meter indications due to electrical noise and to dye fluorescence other than lasing were always smaller than 0.2 watts. A fast photodiode was used to observe the laser output pulse waveform.

The operating procedure in these tests was to choose a dye flow rate and laser pulse rate, snap-start the power supply for immediate laser operation at full power, continue operation long enough to allow the power meter to respond fully, and then immediately stop operation to allow cooling of the laser components before commencing another run with new operating conditions. This short burst operation was necessitated primarily by a lack of flashlamp electrode cooling, which leads to melting of the electrode structure if high power operation is continued for more than a few seconds. Redesign of the electrode assembly to obviate this problem is now underway.

Some results of the laser tests are shown in Fig. I-3 to I-5. The laser pulse waveform, displayed in Fig. I-3, is similar to that observed in earlier tests without the series spark gap. As in the earlier tests, the duration of the laser output pulse (1.7 microsecond, FWHM) is substantially less than that of the corresponding flashlamp output (approx. 2.3 microsecond: see Fig. I-1), due apparently to a quenching of the laser oscillation toward the end of the pulse. This quenching is thought to result from a combination of thermo-acoustic distortion and triplet absorption effects and is presently being investigated. Total energy in the laser pulse is about 10 to 12% less than that obtained without the series spark gap, under otherwise identical conditions.

Fig. I-4 shows the dependence of average laser output power on dye flow rate for repetitive pulsing at various repetition rates. Input energy was 196 joules per pulse at low pulse rates, dropping off by about 5% at 100 pps as described above. In general the laser output is seen to increase with increasing dye flow rate over the flow range employed here. At low pulse rates the output increase levels off at moderate flow rates, suggesting nearly complete interpulse repacement of dye in the active region. However, at 100 pps the laser output is still increasing substantially with increasing dye flow rate even at the highest available flow rates. Although the maximum dye flow (0.63 liter/sec) corresponds to a nominal dye change rate of about 166 sec^{-1} in the 3.8×10^{-3} liter active dye cell volume, it appears that even faster flow is required to clear dye from the cell wall boundary layers.

Fig. I-5 shows the average laser output power as a function of pulse repetition rate at the maximum dye flow rate of 0.63 liter/sec. The power increase vs pulse rate departs somewhat from linearity even at relatively low rates but still increases substantially with increasing rate up to about 100 to 110 pps. At higher pulse rates the laser power actually begins to decrease with increasing rate due to the previously noted power supply limitations as well as the inadequate dye flow rates. However the maximum measured power of 30 watts represents a substantial increase over previously measured levels and over all known published results to date. It appears clear that higher power can readily be obtained if increased dye flow is provided. In addition it should be noted that at no time during these tests were new dye, new spherical pump cavity reflectors, and a new quartz lamp envelope available simultaneously. Unfortunately, all these tend to degrade rather substantially, especially during high power operation. The aluminized spherical reflectors tend to become cloudy and pitted, especially following catastrophic lamp failure, the lamp envelope develops absorbing color centers due to UV irradiation, and the dye appears to degrade noticeably even after only a few thousand shots of high power operation, though the reason for this is not yet known. Based on experience gained in the present tests, it is felt that if all these elements were replaced

FIG. I-3

LASER OUTPUT PULSE – – 140 JOULE INPUT

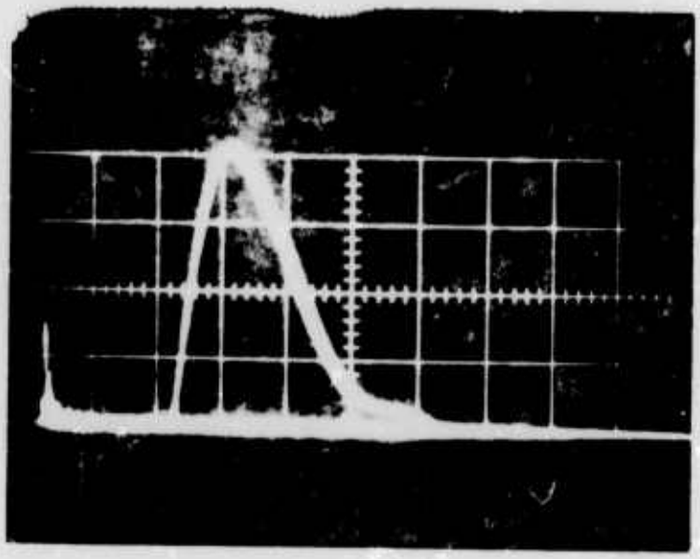

1.0 μsec/div ⟶

N921617–5

FIG. I–4

LASER POWER OUTPUT VS DYE FLOW RATE

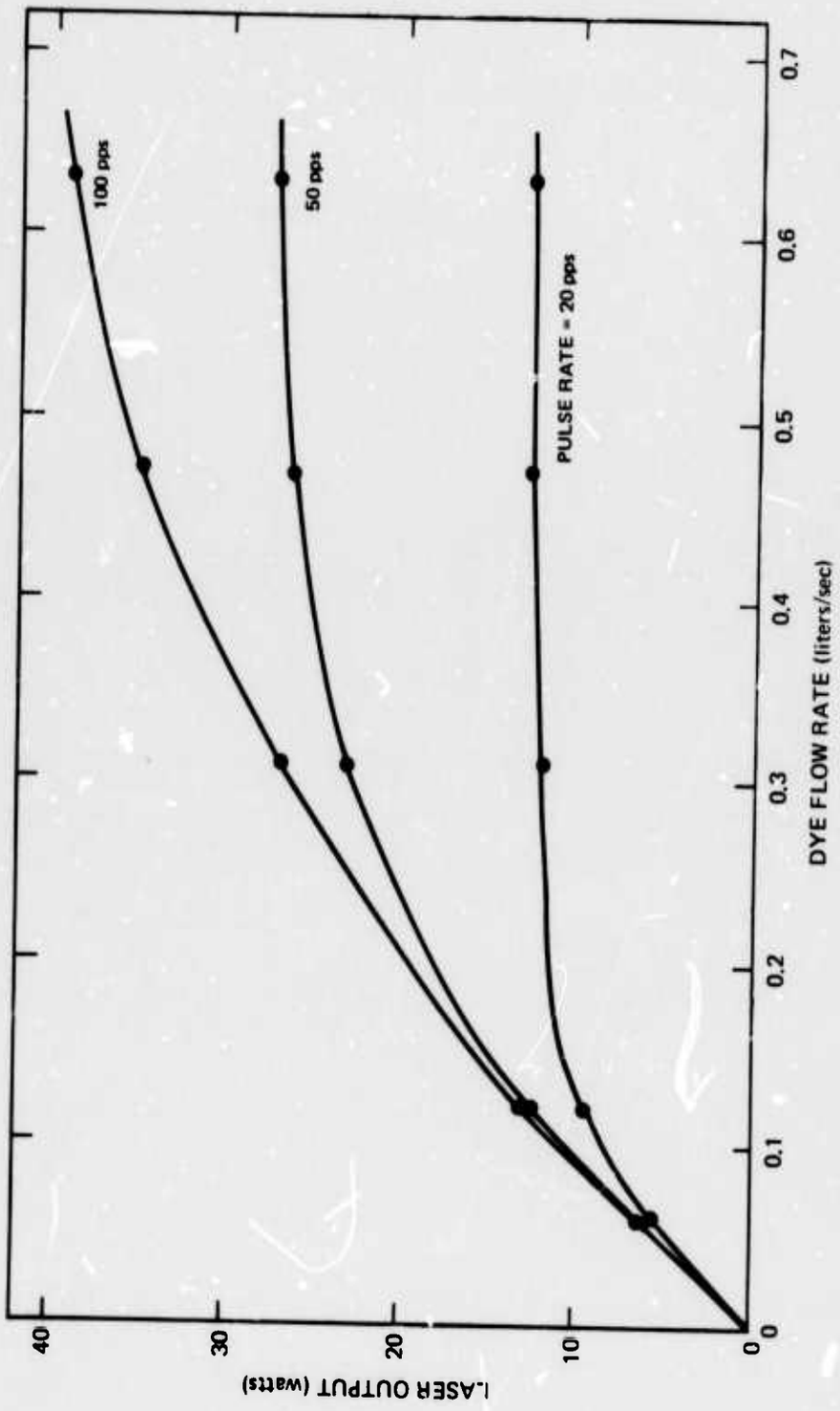

N02-144-1

N921617-5

FIG. I- 5

LASER POWER OUTPUT VS PULSE REPETITION RATE

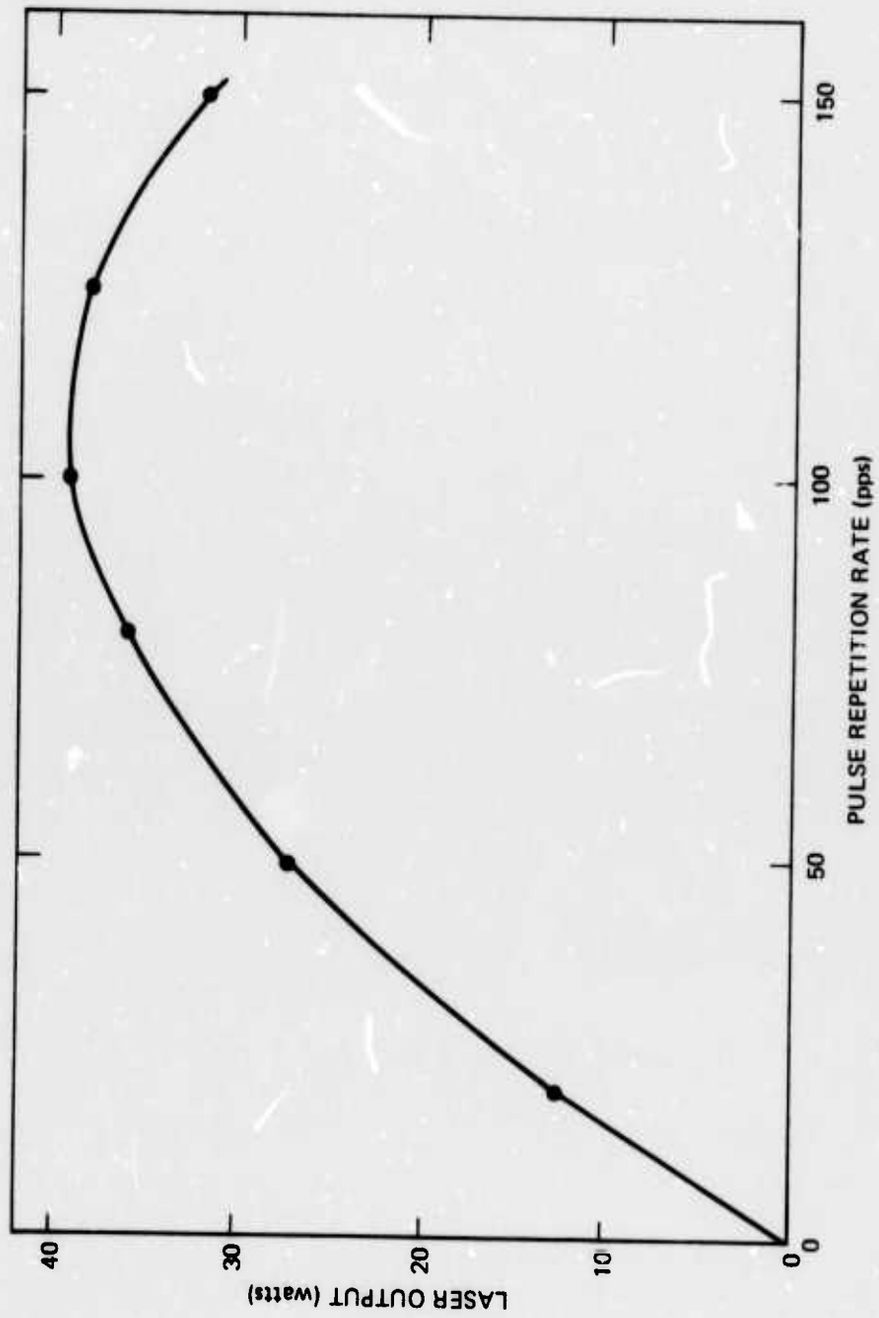

N02-144-5

simultaneously with new ones, laser power in excess of 50 watts could likely be obtained even without increased dye flow. However, to sustain such power for more than a few thousand shots, even on an intermittent operating schedule as used in these test, appears to require use of high purity quartz lamp envelopes to reduce color center formation, possible overcoating for protection of the aluminized reflector surfaces, and increased dye reservoir volume or other means of minimizing dye degradation problems.

1.3 Conclusions

Flashlamp self-firing problems at high repetition rates have been eliminated by adding a series spark gap to perform the necessary high voltage switching function. The value of the series switch technique has been shown by using it in operating the flashlamp at input powers as high as 24 kw and in producing dye laser output powers up to 30 watts. Limitations of the series gap are not yet well-defined. Pulse rates at least to several thousand pps do not seem unreasonable for a well designed gap. However, improvements of the flashlamp and laser will be required to take advantage of such high pulse rates. For example, lamp envelope darkening and explosion problems, electrode, lamp envelope and dye cell cooling techniques, dye flow and dye degradation limitations, cumulative thermo-acoustic distortion effects, etc, will all require considerable attention. If all problems can be overcome to the extent that even higher pulse rates become feasible, it may be desirable to consider replacement of the presently employed series spark gap by a more sophisticated switching device, such as a high power thyratron. However, since thyratrons of sufficiently high current and power ratings are not now readily available, and since the series gap itself seems to offer considerable promise, it is anticipated that laser and flashlamp development work in the near future will continue to make use of the series spark gap technique.

SECTION II

FREQUENCY SWEEPING OF THE DYE LASER

2.1 Introduction

In many high-power dye laser applications it would be desirable to obtain time resolution that is better than that provided by the pulse duration of the present dye laser. One alternative would be the use of a shorter pulse. Shorter duration pumping sources can and have been built. Shortening of the pulse duration generally results in a higher color temperature for the arc and a resulting loss in overall system efficiency. A number of possible schemes to obtain a short effective time duration by imposing a modulation on the output of the laser have been considered in Ref. II-1. It is shown there that an attractive solution involves operating the dye laser with a narrow linewidth and sweeping the linewidth over a much larger spectral range during the duration of the output pulse. The swept pulse can subsequently be compressed to yield a much shorter pulse duration. The situation is somewhat similar to the pulse compression technique used in microwave radar; it differs in that the optical carrier frequency is not processed coherently. The effective pulse compression that can be achieved is given by the ratio of the total spectral width covered to the instantaneous linewidth. If a dye laser is operated with a 1 Å linewidth and is swept over a linewidth of 100 Å in one microsecond, a pulse compression of 100:1 can be obtained. This would give an effective pulse duration of 10 ns. In order to investigate the feasibility of this mode of operation, a fast scan interferometer has been constructed and the results obtained to date are described below.

Relatively low finesse (20 to 30) etalons have been used to narrow the linewidth of flashlamp pumped dye lasers. The experimental results show that the laser linewidth can be narrowed to less than 1 Å by using two such etalons (Ref. II-2). Tuning of the laser output by tilting the etalons has also been demonstrated in previous experiments. Due to obvious physical limitations, rapid tuning of the dye laser by tilting an intracavity etalon is not practical. Etalon tuning can also be done by varying the distance between the parallel reflecting surfaces which make up the etalon. Thermal tuning is much too slow. Another possibility is to make the solid etalon from an electrooptic material. With a proper choice of crystal orientation and placement of electrodes, the distance between the parallel faces of the crystal could be made to increase or decrease by varying an applied electric field. This method of etalon tuning has a limitation which arises from the small thickness (a few mm or less) of the requisite etalon. Whether a transverse or a longitudinal field is applied to the thin etalon there is a problem of voltage breakdown. The use of a solid etalon made from a piezoelectric material suffers from the same problems as an electrooptic material.

The problems of tuning a solid etalon can be circumvented by the use of an air etalon in which one mirror is fixed and a second parallel mirror is mounted to a piezoelectric tube. Commercially available scanning Fabry-Perots are made in this way. Mechanical displacement is achieved by piezoelectric expansion and contraction of the electrically driven tube and the difficulty of having to use very high voltages to obtain sufficiently large displacements is overcome by driving the tube at its mechanical resonant frequency (Ref. II-3). For a given applied voltage, the resonant displacement amplitude is larger than the static amplitude by a Q factor which in general is 100 to 400. Such a resonant-driven Fabry-Perot interferometer was constructed and initial testing revealed that it is possible to scan one free spatial range in approximately 0.5 μsec with a peak drive of 30 V. Testing of the fast scan interferometer intracavity to a pulsed dye laser showed it is possible to scan the output over greater than a 100 Å range during a single pulse (0.5 μsec FWHM and 1.5 μsec basewidth).

In Section 2.2, factors which influence the performance of a fast scan interferometer will be considered. In addition, details of the construction and initial testing of the interferometer will be discussed. In Section 2.3 the experimental results of frequency sweeping the output of a dye laser by the fast scan interferometer will be presented.

2.2 Fast Scan Interferometer

Construction of the interferometer, shown schematically in Fig. II-1, follows closely that first reported by Cooper and Greig (Ref. II-3) and later improved by Brannon and Bacon (Ref. II-4). The etalon reflecting surfaces consists of two 1 in. diameter fused quartz optical flats. Three pair of flats were available; one pair coated for 85 percent reflectivity at 6,328 Å was used in the initial testing and checkout of the interferometer, a second pair coated for 85 percent reflectivity at 5,900 Å, and a third pair with the front surface coated for 50 percent reflectivity at 5,900 Å and the rear surface anti-reflection coated. One optical flat is bonded to the end of a Gulton Industries lead zirconate titanate piezoelectric tube. The low loss tangent and the relatively high mechanical Q of the material makes it suited for the application. Mechanical displacement of the optical flat is achieved by piezoelectric expansion and contraction of the tube which is excited in the lengthwise mode by a sinusoidal voltage applied between the inner and outer metallized cylindrical surfaces.

The amplitude of displacement along the resonant length is given by

$$y(x,t) = y_o \sin\left(\frac{\pi x}{\ell}\right) \sin\left(\frac{\pi c t}{\ell}\right) \qquad \text{(II-1)}$$

FIG. II-1

DIAGRAM OF FAST-SCAN FABRY-PEROT INTERFEROMETER

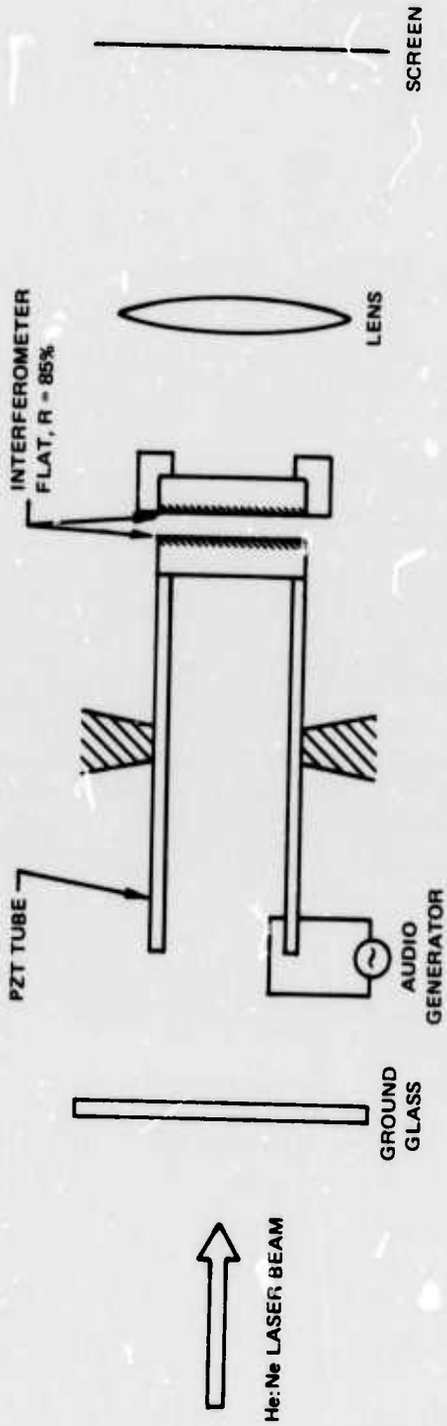

where ℓ is the length of the tube and c is the velocity of sound in the lead zirconate titanite. At any time t, the separation d between the Fabry-Perot plates is:

$$d = d_o + y_o \sin \frac{\pi c t}{\ell}, \qquad \text{(II-2)}$$

where d_o is the static separation. Then,

$$\frac{\Delta d}{\Delta t} = \frac{y_o \pi c}{\ell} \cos\left(\frac{\pi c t}{\ell}\right). \qquad \text{(II-3)}$$

For each $\Delta d = \lambda/2$ extension of the PZT tube, the interferometer scans one free spectral range in a time given by

$$\Delta t = \frac{\lambda \ell}{2\pi y_o c} = \frac{\lambda}{4\pi y_o f}. \qquad \text{(II-4)}$$

where f is the mechanical resonant frequency of the PZT element and λ is the wavelength of incident light. At resonance the total tube extension for a given applied voltage is proportional to the tube length and f, the resonant frequency, inversely proportional to the tube length. Thus, the minimum time required to scan one free spectral range is independent of tube length but depends only on the amplitude of the drive voltage and the Q of the PZT tube. To minimize the decrease in Q by the holding structure, the tube mirror assembly is held at the center of mass, which is a mode of vibration, by a nylon ring which is clamped securely to the tube. A complete assembly is shown in Fig. II-2. Experimentally, it is found that only for short tubes (on the order of 3 cm length, or less) does the clamping ring significantly decrease the Q of the PZT element. On the other hand, long PZT tubes (on the order of 7.5 cm or longer) are undesirable since it is difficult to hold good alignment and spurious resonant modes tend to be excited. The choice of tube length is essentially a compromise between a decreased Q value with short tubes and difficulty of maintaining alignment with long tubes. We find a tube of approximately 4 cm length and a resonant frequency of 40 to 50 kHz is a good compromise between these two conflicting factors.

The primary factors which determines the static (i.e., non-scanning) finesse of the interferometer are (assuming perfect alignment of the optical flats):

FIG. II-2

PZT UNIT

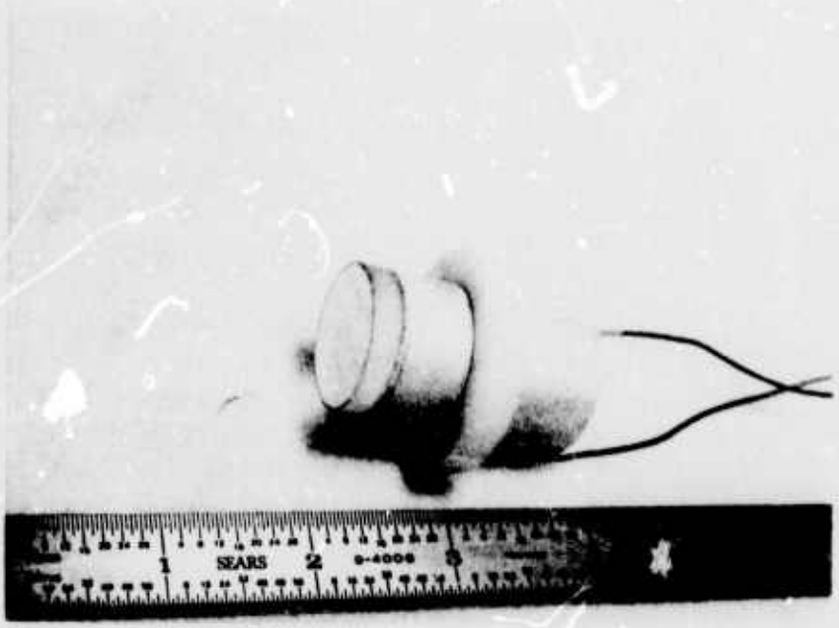

$$F_R = \text{Reflectivity Finesse} = \pi\sqrt{R}/1-R$$
$$F_{SF} = \text{Surface Figure Finesse} = \tfrac{1}{2}\,\frac{1}{SF} \qquad \text{(II-5)}$$
$$F_D = \text{Diffraction Finesse} = 2D^2/\lambda$$

where: R = Mirror reflectivity
SF = Mirror surface figure in wavelength units
D = Aperture diameter
λ = Wavelength of incident light.

Because it is a property of the optical flats, F_{SF} in the "limiting finesse", i.e., if the plates are flat to $\lambda/50$, the maximum instrument finesse is 25.

The dynamic (i.e., the scanning) finesse is degraded by inertial bowing of the moving plate which essentially is a decrease in the surface figure of the plate. An estimate of the magnitude of the bowing can be made using the results of Cooper and Greig (Ref. II-3). Consider a quartz plate 2.5 cm in diameter and 0.95 cm thickness (such as are used in the experiments) which has its outside edge rigidly attached to the end of a thin-walled, cylindrical tube. The tube length is chosen to resonate at 50 kHz and the maximum axial displacement of the quartz plate is 2.5 λ (i.e., 5 fringes are scanned on either side of the equilibrium position). The decrease in surface figure over a 0.2 cm diameter aperture is approximately $\lambda/60$ and the finesse due to this factor alone is approximately 30.

The total instrument finesse is given by:

$$\frac{1}{(F_t)^2} = \sum_i \frac{1}{(F_i)^2} = \frac{1}{F_R^2} + \frac{1}{F_{SF}^2} + \frac{1}{F_D^2} \qquad \text{(II-6)}$$

where for a scanning interferometer F_{SF} is determined by the mirror surface figure with no scan and the inertial bowing of the mirror while scanning. In practice, the interferometer aperture is sufficiently large to make the diffraction finesse negligible. A plot of the interferometer finesse as a function of mirror reflectivity with the mirror surface figure as a parameter is shown in Fig. II-3. It is apparent that for mirror reflectivities less than approximately 70 percent, the total instrument finesse is determined largely by the mirror reflectivity and the reduction in finesse due to bowing is important only for mirror reflectivites greater than approximately 85 to 90 percent. A lack of parallelism in the movement of the plate also results in a decrease in the instrument finesse. The difficulty of securely holding long PZT tubes, with a resulting decrease in parallelism between the interferometer plates made the long tubes unsuitable for use in the fast scan interferometer.

N921617–5

FIG. II-3

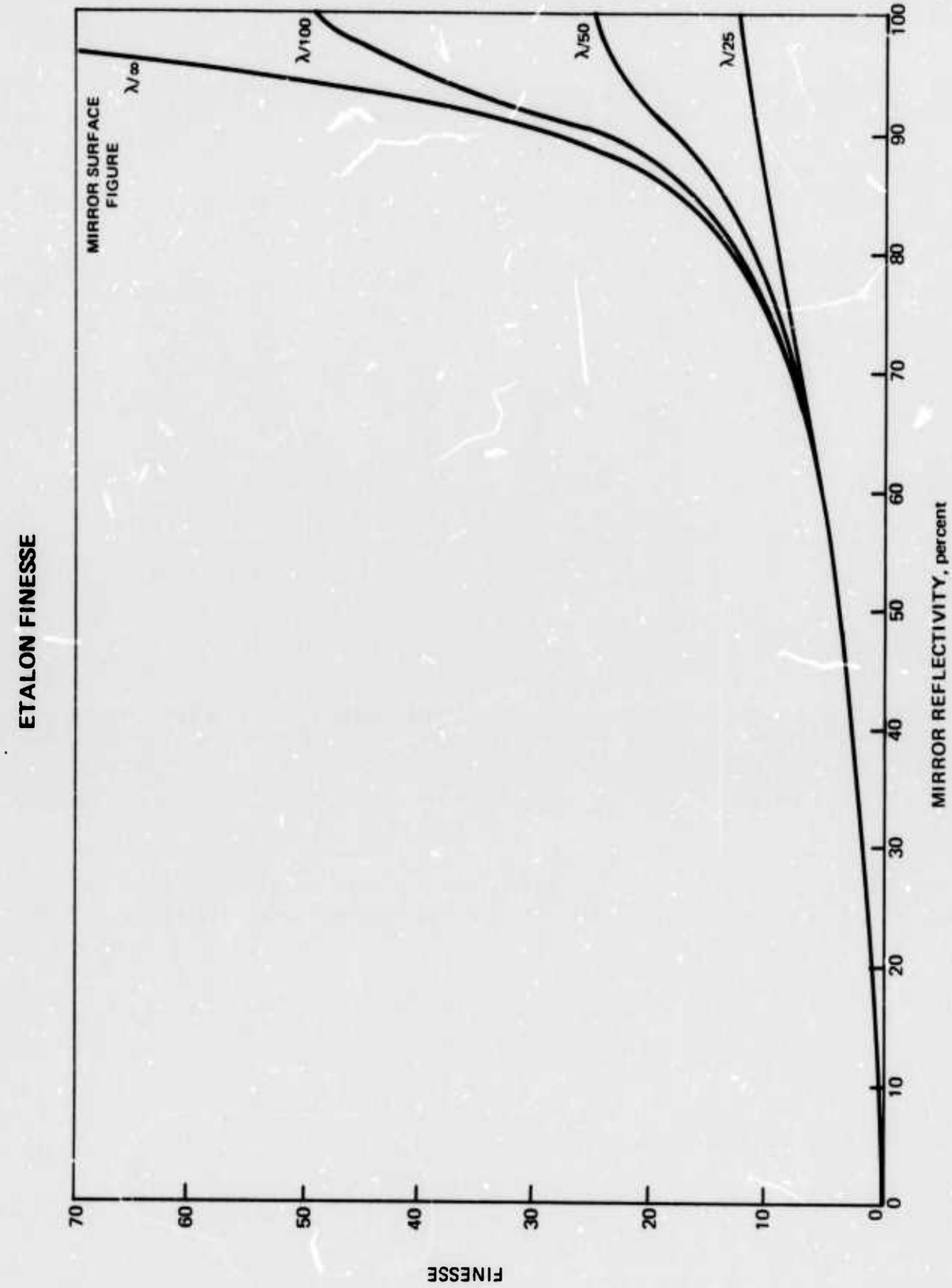

N02-199-9

The complete tube-mirror assembly is mounted in an angular orientation device which has differential micrometer screws for precise angular control of the assembly relative to the second interferometer mirror held in a specially designed mirror mount. This second mirror is mounted on a prevision translation stage which allows control of the mirror spacing (and thus the interferometer free spectral range) to better than 1 micron. Photographs of the complete interferometer is shown in Figs. II-4 and II-5.

Initial testing of the interferometer was done at 6,328 Å wavelength using mirrors coated for 85 percent reflectance. The interferometer parameters of interest are: time to scan one free spectral range, free spectral range and finesse.

The time to scan one spectral range, or the scan time, is measured using the experimental configuration shown in Fig. II-1. Initial alignment of the interferometer (with no scan voltage) is done by adjusting the plate parallelism for minimum fringe width. The ground glass piece is then removed and the viewing screen replaced by a PIN photodiode. The photodiode output and the PZT drive voltage are displayed on a dual channel scope. A number of free spectral ranges are scanned during each half cycle of the drive voltage and a typical display of the interferometer output is shown in Fig. II-6. Each spike represents a scan of one free spectral range and the spacing between the spikes is the scan time. The PZT resonant frequency is easily determined since it results in scanning the maximum number of free spectral ranges for a given drive voltage and a fine frequency adjust is made by varying the drive frequency until the interferometer output is in phase with the PZT drive voltage waveform. Increasing the drive voltage amplitude increases the number of free spectral ranges and decreases scan time. A plot of the scan time as a formation of the peak drive voltage is shown in Fig. II-7 where a 33 V peak drive resulted in a 0.57 μsec scan time and the corresponding resonance frequency of the 3.81 cm long PZT element is 48.2 kHz. The interferometer output at the 0.57 μsec scan time is shown in Fig. II-8 where the nonuniform height of the interferometer output and the decreased finesse at the edges of the scan region are evident. These effects, which are evident only at the higher drive levels, could be due either to bowing or tilting of the moving interferometer mirror. However, maximum finesse is achieved over approximately five free spectral ranges and this is adequate for the dye laser frequency sweeping experiments if proper synchronization between the PZT drive voltage and the dye laser pulse is provided.

The mechanical "Q" factor of the interferometer can be estimated by comparing the drive voltage required to scan one free spectral range with a low frequency drive compared to that at the resonant frequency. A low frequency scan requires 890 V while only 4 V are required at resonance so the "Q" factor is approximately 223.

FIG. II-4

FAST SCAN FABRY–PEROT INTERFEROMETER

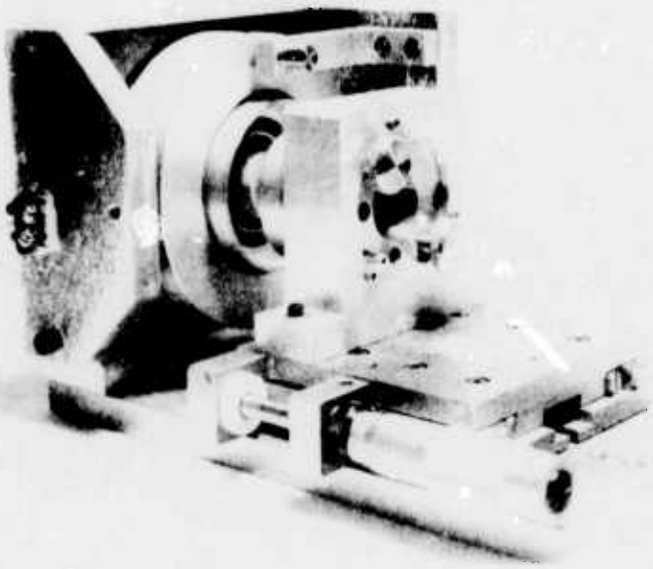

FIG. II-5

FAST SCAN FABRY–PEROT INTERFEROMETER

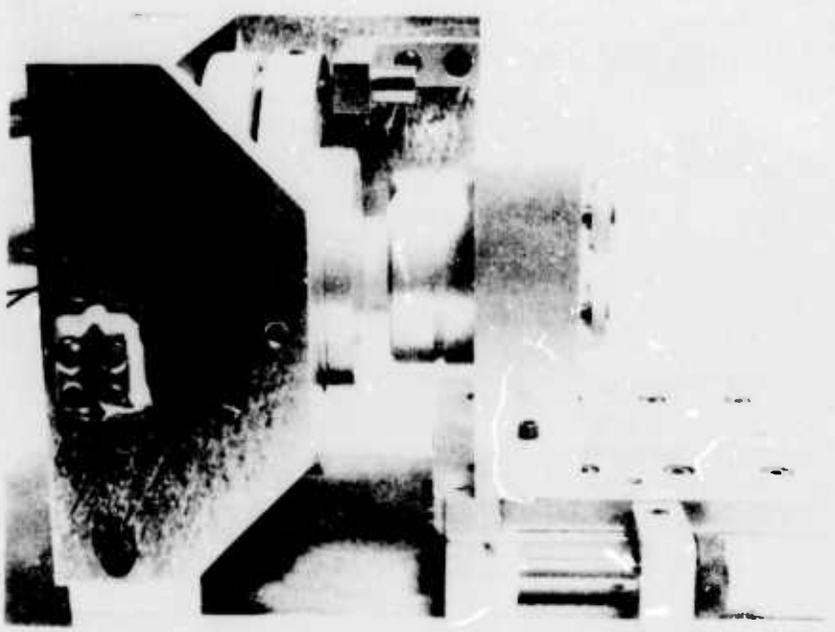

FIG. II–6

FAST–SCAN FABRY–PEROT INTERFEROMETER

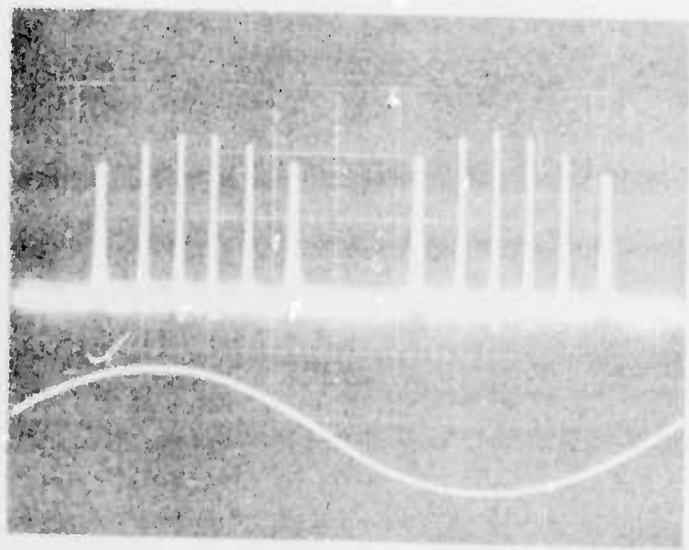

FIG. II-7

FAST SCAN INTERFEROMETER CHARACTERISTICS

$f_o \approx 48.2$ kHz

FSR = 58 Å AT 6328 Å

FSR = 67 Å AT 5900 Å

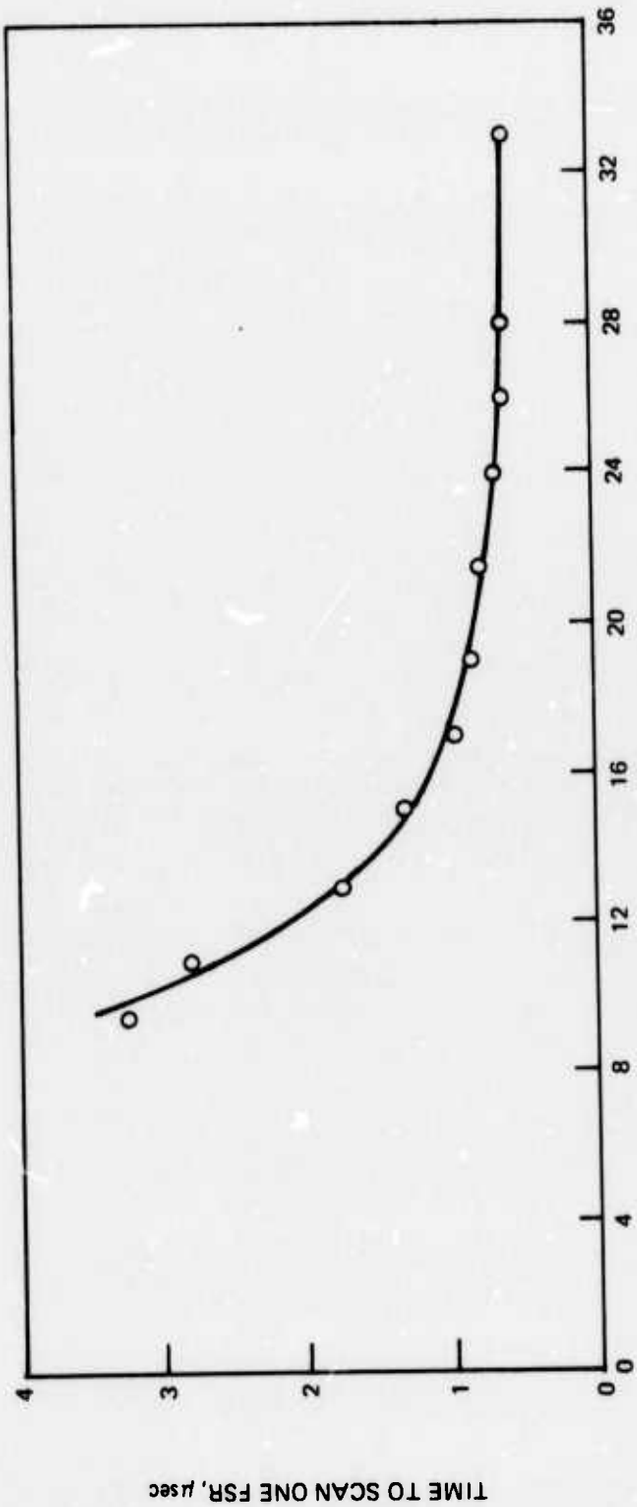

FIG. II-8

FAST–SCAN FABRY–PEROT INTERFEROMETER

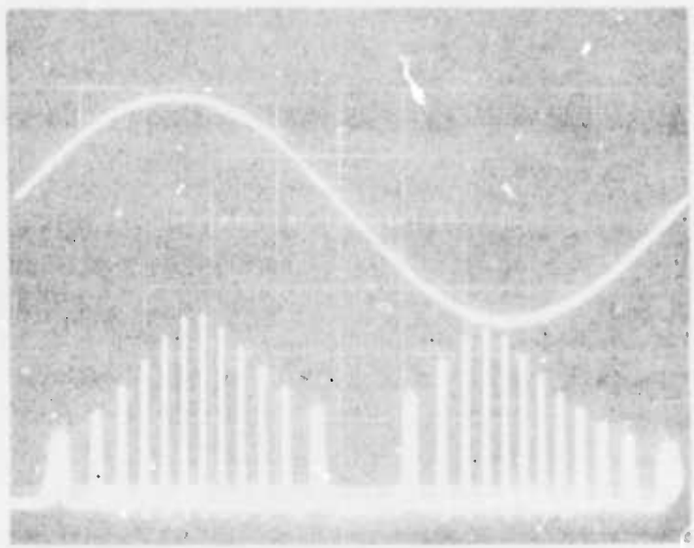

The interferometer plate spacing, and thus its free spectral range, is determined by examination of the resultant fringe pattern, which is formed when the interferometer aperture is illuminated by a spatially broad but monochromatic light source, such as is shown in Fig. II-9. A ray incident on the interferometer at an angle θ is broken into a series of parallel transmitted rays and a lens is required to bring these parallel rays together for interference. The condition for reinforcement of the transmitted rays is given by $2d \cos \theta = m\lambda$, where d is the plate spacing, θ is the angle of the incident ray, m is an integer and λ is the wavelength of the incident light. This condition is satisfied by all points on a circle in the focal plane of the lens. A second, adjacent fringe will appear when $2d \cos \theta' = (m + 1)\lambda$ and the plate spacing can be determined by taking the difference of the two equations and solving for d. The result is

$$d = \frac{\lambda}{2(\cos \theta - \cos \theta')} . \qquad \text{(II-7)}$$

Use the small angle approximation $\cos \theta = 1 - \theta^2/2$ and substitute $\theta = r/f$ where r is the radius of the fringe in the focal plane of the lens of focal length f. The result is:

$$d = \frac{f^2\lambda}{r'^2 - r^2} . \qquad \text{(II-8)}$$

Thus, by measuring the radius of two successive frings in the lens focal plane, the interfereometer plate spacing and thus its free spectral range is determined.

A convenient monochromatic source is the He:Ne laser beam incident on a ground glass screen placed between the laser and the interferometer. A resultant fringe pattern is shown in Fig. II-10. For interferometers with a large free spectral range, which corresponds to a small plate separation, the radius difference between successive fringes becomes large and obscuration of the second order fringe by the mirror holder, etc., beomces a problem. It is then necessary to increase the plate separation by a known amount until a number of fringes are visible, determine the new plate separation from this fringe pattern using Eq. (II-8), and subtract the known increase in plate separation to determine the original separation. This procedure is necessary for a free spectral range larger than approximately 30 Å.

Using this technique, the free spectral range of the interferometer used to obtain the data shown in Fig. II-7 was measured to be 58 Å at 6,328 Å wavelength (or 67 Å at 5,900 Å) and free spectral ranges to 200 Å have been measured. Another convenient method of measuring the free spectral range is to view the dye laser output using a spectrometer when the interferometer is intracavity to the laser, and this method will be discussed below.

FORMATION OF FRINGE PATTERN FROM MULTIPLE REFLECTIONS

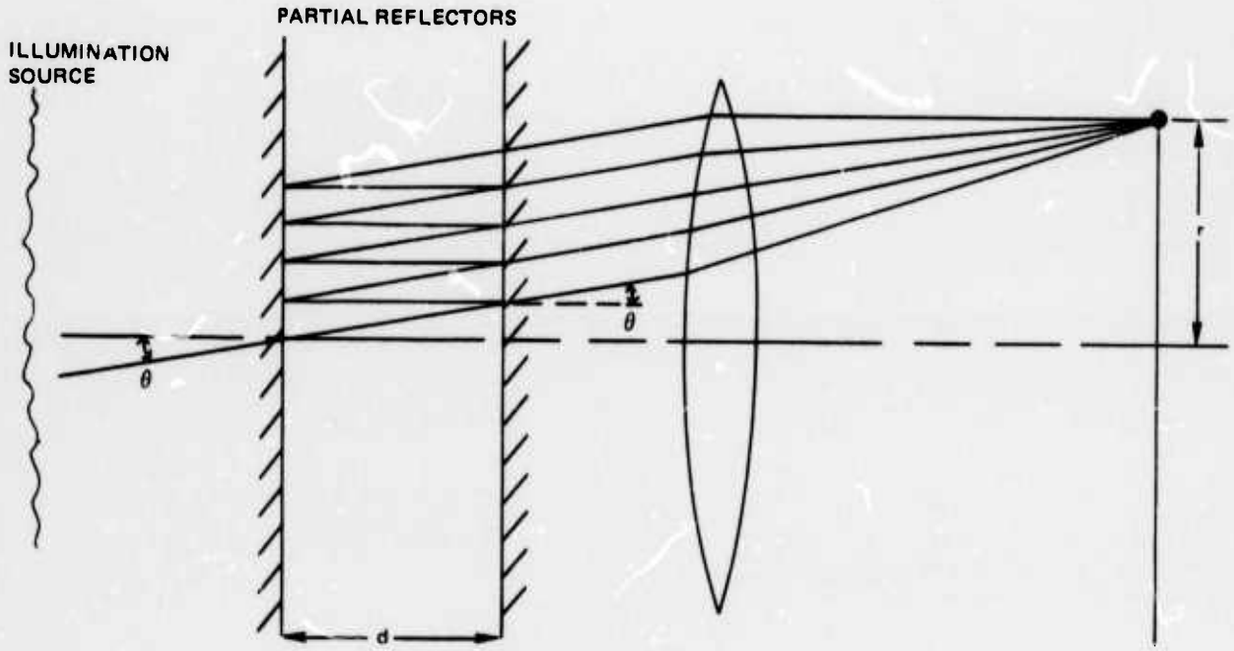

FIG. II-10

FAST-SCAN FABRY-PEROT FRINGE PATTERN

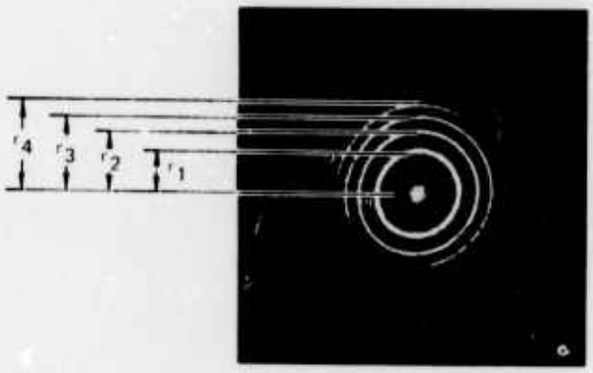

2.3 Dye Laser Frequency Sweep Experiments

The experimental configuration used in the dye laser frequency sweep experiments is shown in Fig. II-11. The dye laser head consists of a Candela CL-100E coaxial flashlamp excited by a low inductance drive circuit consisting of a 0.3 μf capacitor and a triggered spark gap. A typical current drive pulse is 2 μsec (FWHM) with a 50 J input to the lamp. The input was limited to 60 J although the lamp was designed for a maximum of 100 J. A 10^{-4} molar solution of rhodamine 6 G in ethanol was circulated through the flashlamp at a flow velocity of approximately 15 cm/sec. The lamp PRF was limited to one pulse every 10 sec to allow for complete removal of the thermally heat dye and cooling of the discharge lamp between pulses. The laser cavity consists of a 1 m radius maximum reflecting mirror adjacent to the laser head, and a flat output mirror of either 30 percent or 80 percent reflectivity and a mirror spacing of 60 cm.

The diagnostic instrumentation used to examine the laser output consisted of a high-speed PIN photodiode, a Fabry-Perot interferometer and a Jarrell Ash 1 m spectrometer. The diagnostic interfereometer consisted of either a 0.05 mm thick solid etalon (free spectral range 25 Å) or an air etalon with a free spectral range adjustable to 100 Å. The interferometers are used for a quick check of the laser linewidth and to determine frequency sweeping by observing broadening, or complete disappearance of the fringe pattern.

The dye laser pulse and the PZT scan voltage are synchronized using a dual pulse generator with a coarse time delay continuously variable from 0 to 10 msec. Heating of the PZT tube, and therefore possible misalignment of the scanning interferometer is prevented by gating the audio drive voltage for a 10 msec duration. The dye laser pulse is delayed to occur near the end of the drive pulse to assure the PZT was in a resonant condition. An additional fine time delay control allows the dye laser pulse to be positioned at the peak of the PZT drive voltage to assure maximum finesse and minimum scan time of the interferometer (see Fig. II-8).

With no intracavity scanning interferometer and a 30 percent output mirror, the laser output energy was approximately 50 mJ with 60 J input to the flashlamp. A wavelength spectrum and a time display of the laser output, also with no intracavity etalon are shown in Figs. II-12 and II-13, respectively. The laser linewidth is approximately 200 Å centered near 5,900 Å, and the pulse width is approximately 0.5 μsec (FWHM) and 1.5 μsec base width.

Initial operation with the interferometer intracavity to the dye laser showed that 85 percent (at 5,900 Å) mirrors resulted in a high laser threshold and a corresponding low output energy. The laser operation was found to be satisfactory using 50 percent interferometer mirror and an 80 percent reflectivity output mirror. With the intracavity interferometer, the laser output pulse width was essentially

FIG. II--11

EXPERIMENTAL CONFIGURATION

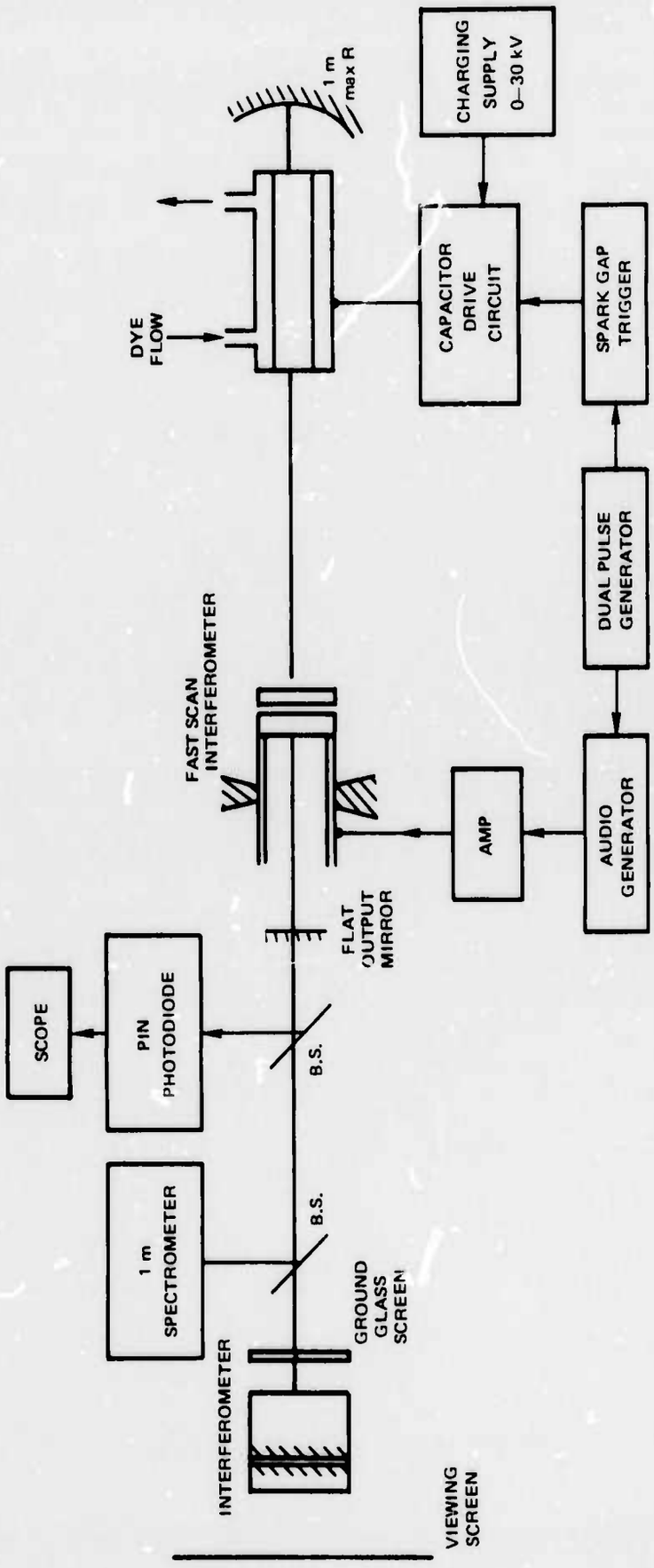

N02-199-6

DYE LASER OUTPUT SPECTRUM

NO INTRACAVITY ETALON

N02–199–3

FIG. II-13

TIME DISPLAY OF DYE LASER OUTPUT

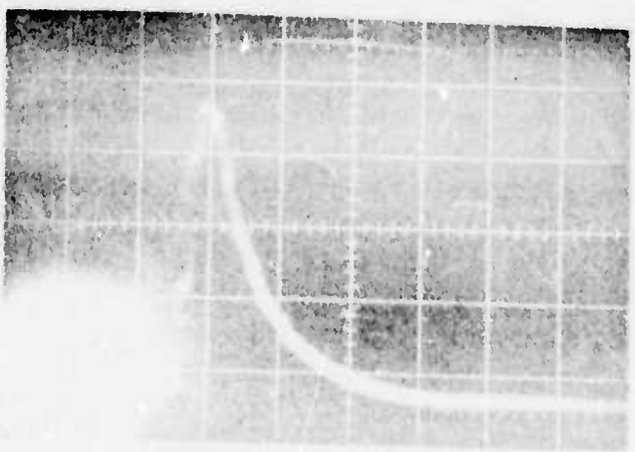

0.5 μsec/div

unchanged from that with no interferometer and the energy output was reduced to 5 to 10 mJ. The corresponding wavelength spectrum of the laser output is shown in Fig. II-14 where the interferometer was adjusted to have a free spectral range of approximately 30 Å and approximately 60 Å (measured using a He:Ne laser and observing the resulting fringe pattern) in the top and bottom photographs, respectively. The dye laser output occurs at the multiple peaks of the interferometer transmission, as is expected, and this measurement is a convenient method of determining the interferometer free spectral range. Increasing the free spectral range further resulted in the spectrum shown in the top photograph of Fig. II-15. This result demonstrates that a single, low finesse intracavity etalon is adequate to substantially narrow the operating linewidth of the dye laser output. Tuning of the laser output by applying a dc voltage to the PZT element of the interferometer, also shown in Fig. II-15, demonstrates the etalon finesse is adequate to control the laser frequency. A quick check on the approximate linewidth of the laser output, and whether it is operating single or multiple line, is also made by viewing the diagnsotic interferometer output; examples are shown in Figs. II-16 and II-17.

Experiments were continued to verify frequency sweeping of the dye laser output with a voltage, at the resonant frequency, applied to the PZT element. The experimental procedure is to adjust the free spectral range of the intracavity scanning interferometer so that the laser output is in a single narrow wavelength range typically 20 Å or less. The drive frequency to the PZT element is then adjusted by passing the output of a He:Ne laser through the dye laser output mirror and interferometer. A removable glass slide beam splitter defects the beam to a PIN photodiode. The frequency adjustment, which was described in the previous section, is done with a pulsed drive voltage to prevent heating, and therefore misalignment, of the interferometer. The beam splitter is then removed. Synchronization of the dye laser and the PZT drive voltage is accomplished by viewing the laser output using a PIN photodiode and the PZT drive voltage on a dual channel scope and adjusting the relative time delay so that the laser pulse occurs at the peak of the drive voltage waveform. Synchronization to approximately 0.5 μsec is possible.

Evidence of sweeping the dye laser output by viewing the diagnostic interferometer output is shown in Fig. II-18 where the voltage indicated is the peak drive to the scanning interferometer PZT element. These photographs do not conclusively prove frequency and a more positive indication is given by observing the spectrometer output; an example of which is shown in Fig. II-19. The laser output with and without a drive voltage to the PZT element are shown in the top and bottom photographs, respectively. With a drive voltage the laser output is scanned approximately 50 Å and a scan over greater than a 100 Å wavelength range is shown in Fig. II-20. The latter photograph illustrates the fact that the scan does not necessarily begin or end at the wavelength of the laser output with no

DYE LASER OUTPUT SPECTRUM

WITH INTRACAVITY ETALON

a) INTERFEROMETER FSR = 30 Å

b) INTERFEROMETER FSR = 60 Å

DYE LASER TUNING

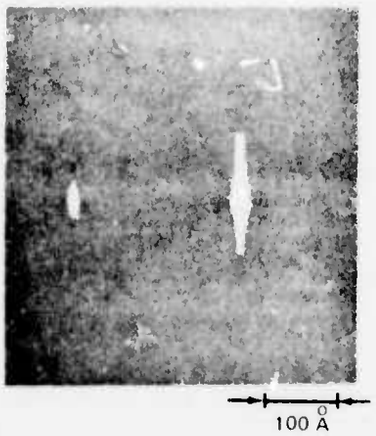

a) ZERO VOLTS

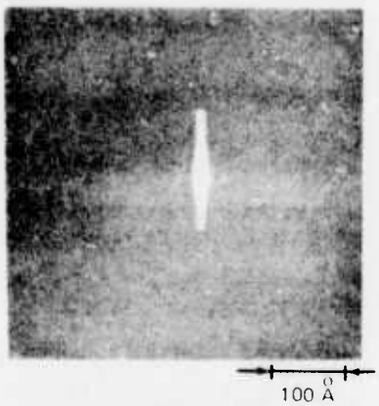

b) 500 VOLTS

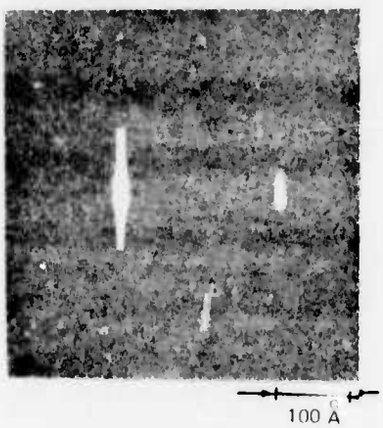

c) 1000 VOLTS

FIG. II–16

DYE LASER SPECTRUM

NO INTRACAVITY ETALON

DYE LASER SPECTRUM

WITH INTRACAVITY ETALON

INTERFEROGRAM OF DYE LASER OUTPUT

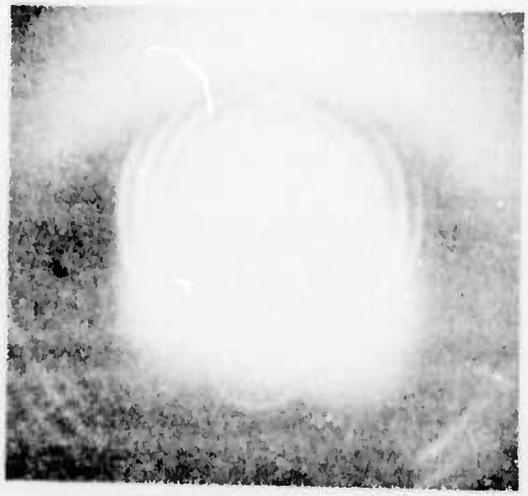

a) 0 V

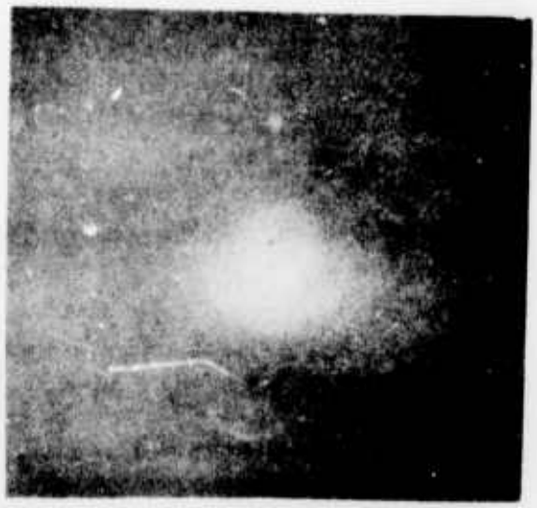

c) 20 V

b) 17.5 V

d) 22.5 V

DYE LASER OUTPUT SPECTRUM

100 Å

a) PZT DRIVE VOLTAGE

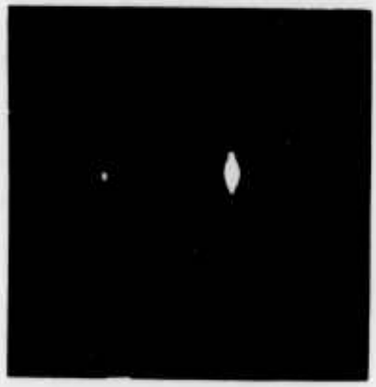

100 Å

b) NO PZT DRIVE VOLTAGE

DYE LASER OUTPUT SPECTRUM

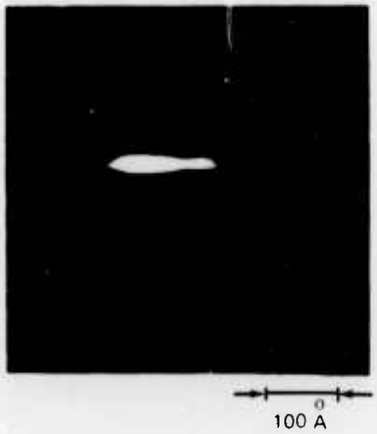

a) PZT DRIVE VOLTAGE

b) NO PZT DRIVE VOLTAGE

drive voltage. The reason for this is primarily due to a time difference between the taking of the two photographs during which the center bandpass of the interferometer can change part is also due to synchronization between the PZT drive voltage and the laser pulse.

The primary problem encountered is the laser output is not swept over a complete free spectral range although the scan time, as compared to the total pulse width, indicates it should be. A good example of this incomplete frequency sweep is shown in Fig. II-19 where the spacing between laser output at two wavelengths indicates the interferometer free spectral range in approximately 150 Å (verified by measurement using the He:Ne laser) but the laser output is swept over a 60 Å wavelength range. A careful examination of the laser output pulse width shows it to be essentially unchanged from that with no sweep. The result implies the scan time of the interferometer needs to be somewhat less than the halfwidth of the laser pulse. Attempts to verify this by lengthening the laser pulse width (by widening the flashlamp pulse width) resulted in a very low laser output and no conclusive results were obtained.

An unusual type of spectrum, which again illustrates that the experimental results are not completely understood, is shown in Fig. II-21 where the output consists of an unswept and two swept parts. The laser may have operated simultaneously or in time sequence in these various modes and time resolution using a streak camera could resolve these differences. The other interesting aspect of the spectrum shown in the top photograph is the spacing between the two swept portions of the spectrum are separated by approximately 250 Å which is well beyond the 150 Å free spectral range of the interferometer.

In conclusion, the most promising techniques to rapidly frequency sweep the output of a pulsed, flashlamp pumped dye laser was judged to be a resonant driven air spaced Fabry-Perot interferometer. Such an interferometer was constructed and initial tests revealed that it is possible to scan one free spectral range in approximately 0.6 μsec with a peak drive of 30 V at 48 kHz. A free spectral range to 150 Å has been achieved and 200 Å is believed to be the practical limit. Testing of the fast scan interferometer intracavity in a dye laser showed it is possible to scan the output over greater than a 100 Å range during a single pulse (0.5 μsec FWHM and 1.5 μsec base width). The linewidth of the laser output with no scanning is typically 20 Å; however, with addition of a second etalon could be narrowed to approximately 1 Å. To achieve a narrow instantaneous linewidth during scanning would require a second scanning etalon or other narrowing scheme. This will be the object of further work. It appears feasible to obtain 100-200 resolution points.

FIG. II- 21

DYE LASER SPECTRUM

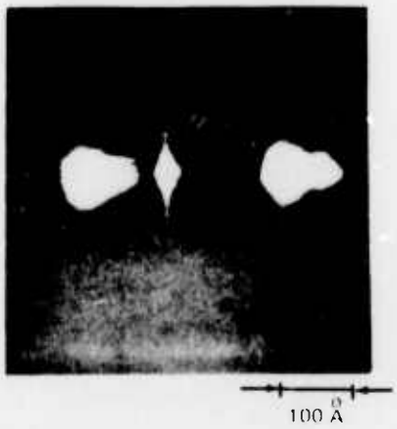

a) PZT DRIVE VOLTAGE

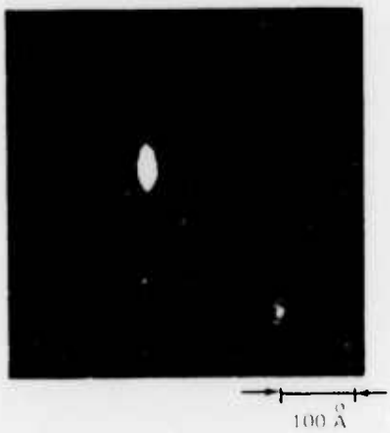

b) NO PZT DRIVE VOLTAGE

N02-100-4

REFERENCES

II-1. United Aircraft Corporation Research Laboratories Report P-L252; Proposal For the Development and High Power Dye Laser Technology (1972).

II-2. Gale, G. M.: Optics Communications, 7, p. 86 (1973).

II-3. Cooper, J. and J. R. Greig: J. Sci. Instruments, 40, p. 433 (1963).

II-4. Brannon, P. J. and F. M. Bacon: Applied Optics, 12, p. 142 (1973).

SECTION III

HIGH ENERGY VORTEX STABILIZED FLASHLAMPS

3.1 Introduction

When energies greater than 225 joules are discharged in the present vortex stabilized flashlamp there is a good chance of producing a catastrophic rupture of the thick walled fused quartz containing vessel that confines the gas vortex and arc. One proposal considered to allow for higher discharge energies was to remove the quartz containing vessel and its surrounding grounded cage return in the present lamp and produce a vortex along the electrode axis by a tangental injection of gas along the diameter of the laser pumping cavity sphere. With this scheme the intense shock wave produced by the arch discharge would be more easily dissipated by the larger volume of the sphere. In addition to allowing for higher discharge energies, it was thought that the unconfined vortex could stabilize the discharge with a much smaller flow of gas because of the removal of the gounded cage return that closely surrounds the present arc. A prototype rig to test the unconfined vortex was constructed from spare parts and has been described in a previous UARL technical proposal.(Ref. III-1) Pressure measurements made in the sphere and discussed in the proposal demonstrated the ability of the gas injection scheme to produce a good vortex and corresponding pressure drop along the interelectrode axis. The present discussion will be concerned with tests and observations made on different arc discharges in the prototype rig with gas flow rates up to 36% of that used in the present vortex flashlamp.

3.2 Arc Discharges in Test Rig

The lower electrode that extends 1.25 cm inside the bottom of the reflecting sphere was electrically insulated from the adjacent sphere on the outside with a lucite annular disc. Internally several schemes were used to insulate the lower electrode from the grounded sphere to which the upper electrode was connected. Initially a glass dish was constructed as a bowl with a stem that surrounded the lower electrode about 1 cm away and was cemented in place with RTV. The breakdown of a small capacitor between the electrodes when using pure Argon produced a discharge that jumped the can gap to the glass dish and spreading in many directions ran up the side of the dish to the sphere. A few different insulating glass collars were tried and had only marginal success. The upper electrode was then insulated from the sphere along the supporting struts that run the diameter of the sphere. The sphere was allowed to electrically "float". Even with the latter arrangement the discharge would occasionally go up the walls of the sphere and along the struts. The discharging along the surfaces instead of between the electrodes was eliminated by the addition of about 5% CO_2 gas to the Argon flow. With the Argon/CO_2 gas mixture the glass collars and dish could be eliminated and the discharge

took place between electrodes. The discharge, however, was highly unstable as shown by Fig. III-1 which is a photo of several discharges. The discharge or arc instability was present even at the maximum allowable 15 psig inlet pressure on the vortex jets. This corresponds to a gas flow rate of 1.8 ℓ/sec (measured by a Fisher-Porter flow-meter) as compared to 5 ℓ/s for the present vortex lamp. From previous data[1] on the pressure drop at the electrode axis, a flow rate of 1.8 ℓ/s gives only a 2.9% drop in the total pressure (or gas density) on the electrode axis in the prototype rig. To obtain the 37% drop in total pressure which was measured in the present vortex lamp[2] (Ref. III-2) would require a flow rate of about 7 /s for the prototype rig. The inlet pressures required for this flow are too large for the present test rig and its connecting tubing. To obtain these flow rates the prototype would require larger diameter inlet jets and a sturdier attachment of the two hemispheres to support the increased pressures.

There is no reason to believe that higher gas flows would not stabilize the arc in the prototype as in the present vortex lamp. The advantage for the unconfined vortex alone to stabilize the discharging arc at slower flow rates, however, does not seem realizable in view of the present results.

3.3 Arc Stabilization at High Repetition Rate

An interesting observation was made when the CO_2 additive gas was replaced by N_2. With 5 to 10% N_2 mixed in with the Argon flow the discharge was unstable as usual for the first few shots and then would run at a high repetition rate as a relaxation oscillator. The discharge would appear to "lock on" to the interelectrode axis as it broke into high repetition rate operation. Observation of the light output with a photodiode indicated a nearly perodic discharge rate at about 200 Hz. This agrees with the RC time constant of the discharge capacitor. The repetitive "locked on" discharge was quite stable along the electrode axis except for a small reoccuring wiggle of insignificant magnitude. Figure III-2 shows a typical example of the discharge locking on to the electrode axis. In this photo 3 unstable discharges took place before the system locked on to the axis. The unstable discharges take place between the edges of the electrode exit holes while the stabilized high repetition rate discharge continues far down into the exit holes. It was also observed that the high repetition rate discharge would remain stable for gas flows as low as a few tenths ℓ/s.

The stabilization of the arc discharges at high rather than low rep. rate means that a dc discharge would also be stable on the interelectrode axis. This idea was tested by removing the discharging capacitor and indeed found to be true. The dc discharge could be used as a guide or sustainer current to stabilze a large pulsed discharge from a capacitor. Figure III-3

FIG. III-1

UNSTABLE 1J DISCHARGES IN TEST RIG

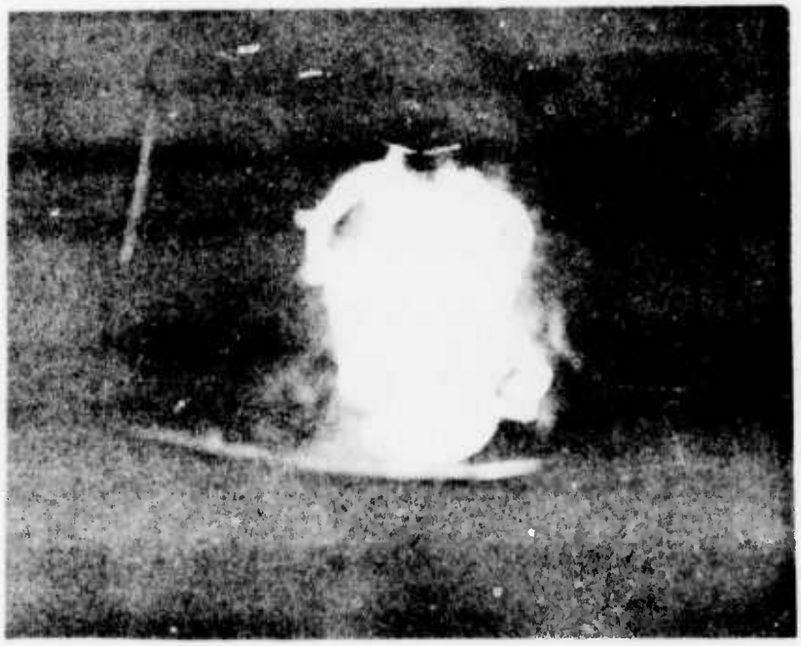

N02-195-1

FIG. III– 2

ARC DISCHARGE LOCKING ON TO THE INTERELECTRODE AXIS

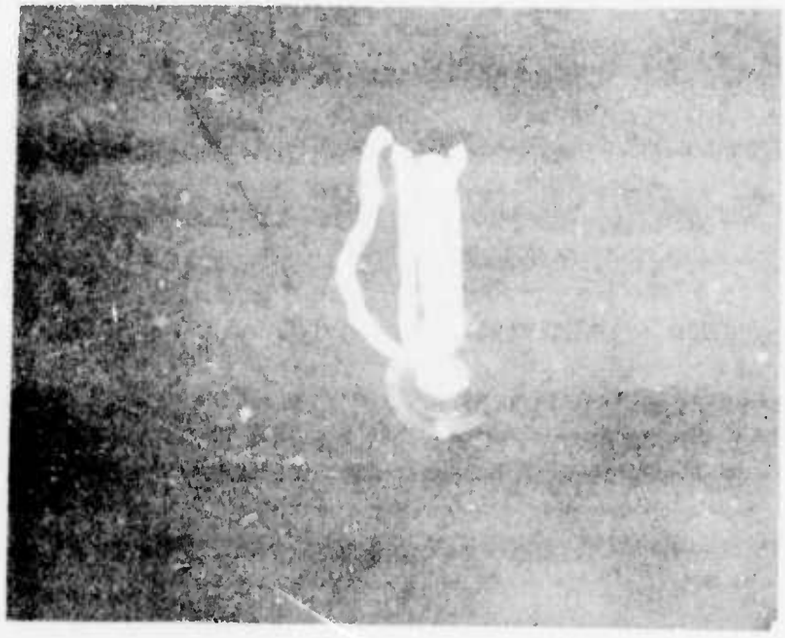

FIG. III-3

SCHEMATIC OF DC SUSTAINER STABILIZED DISCHARGE CIRCUIT

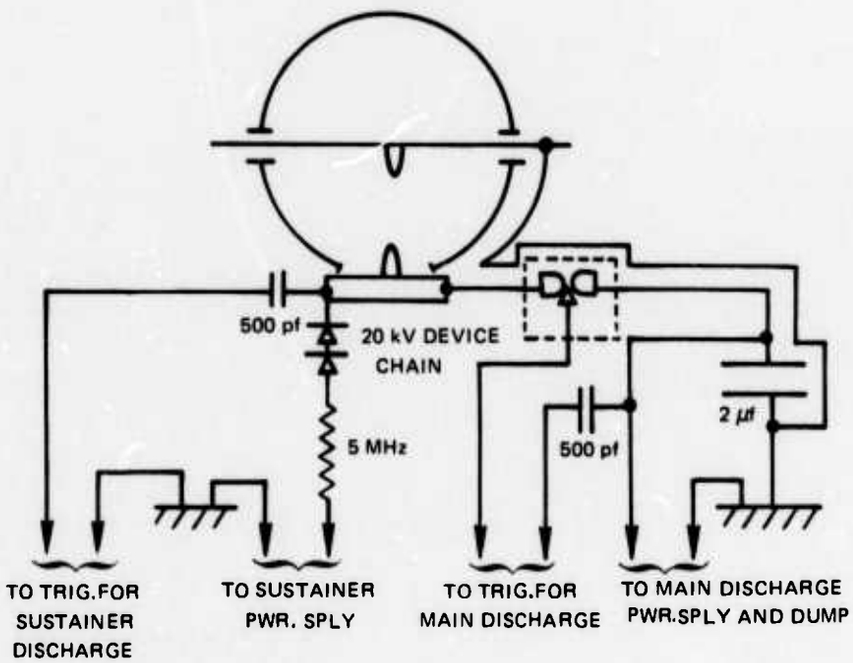

a schematic of the circuit used to test the guided discharge idea. As shown in the schematic, a series spark gap is placed in the flashlamp circuit to isolate the discharge capacitor since the sustainer brings the anode essentially to ground potential. The power supply for the sustainer is isolated from the main discharge with a 20 kv diode rectifier chain. To hold the sustainer current to reasonable values a 5 Mr resistance is placed in series with the power supply. A trigger pulse was also connected in parallel to the flashlamp for initiation of the dc discharge if needed. Figure III-4 shows a picture of the sustainer discharge. Optimum Ar/N_2 mixture ratios for easy ignition of the sustainer were between 2 and 5% N_2 in Ar. For an unknown reason the ignition voltage of the sustainer was quite variable and could lie anywhere between 12 and 18 kv. Flow rates required for stabilization were as low as a few tenths ℓ/s. It was interesting to note that the sustainer could not be ignited in Ar/CO_2 mixtures. Figure III-5 shows a picture of 117 J discharge dumping into the dc sustainer arc. The discharge, which is guided by the sustainer, is straight and on the axis of the electrodes as desired.

The possibility for using the stabilized sustainer discharge for repetitive lamp firings was tested cut by placing another capacitor and series spark gap combination in parallel with the capacitor and spark gap in Fig. III-3. Using a delayed trigger generator the two spark gaps and hence the two capacitors could be fired sequentially with time intervals adjustable from 10 to 10^{-4} sec. The stabilization or straightness of the two discharges was observed visually through a devise red filter. The criterion for the stabilization of the second arc discharge was the allowance of sufficient time for the dc sustainer to reform and stabilize itself. Figure III-6 shows a photo of two discharges triggered 1 sec apart. In this instance both discharges are stable. When the time interval is reduced to 0.1 sec and 0.01 sec the second discharge becomes highly unstable, appearing to follow streamers sent out by the sustainer trying to reestablish itself along the axis. A typical photo of the sequential discharges with a 0.1 sec interval is shown in Fig. III-7. The gas flow rate used for these tests was about 0.8 ℓ/s. 117J was discharges on the first shot and 204J on the second. If the sustainer voltage was reduced after ignition to between 10 and 12 kv the sustainer would be blown out by the first discharge and this would prevent the second discharge from occuring. It appears, then, that the large pulsed discharges are disrupting the vortex for periods in the order of a few tenths of a second. The interruption period could probably be reduced with much larger gas flow rates. Figure III-8 shows a photo of two discharges with a 1 msec time separation. In this instance it appears like the discharge is diffusing over to the sphere at the bottom electrode.

To test the unconfined vortex lamp at a high repetition rate an external spark gap was connected in series with a .02 μf capacitor and the flashlamp. With 2 J discharges and gas flow rates of .8 ℓ/s it was observed that the arc

FIG. III-4

DC SUSTAINER DISCHARGE IN TEST RIG

A STABLE 117J DISCHARGE USING THE DC SUSTAINER

FIG. III-6

TWO DISCHARGES TRIGGERED 1 sec APART

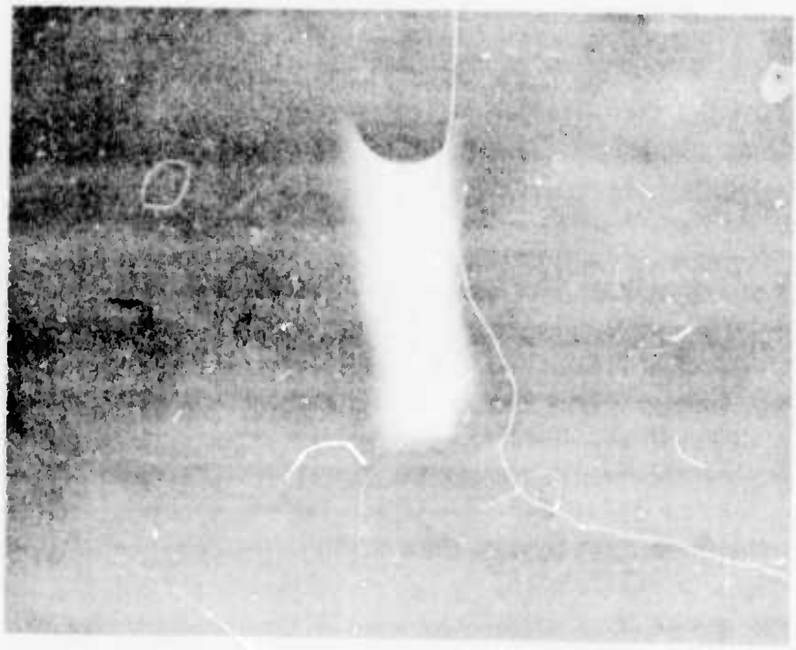

TWO DISCHARGES TRIGGERED 0.1sec APART

FIG. III-8

TWO DISCHARGES TRIGGERED 1 msec APART

was highly unstable for repetition rates up to 100 Hz. Above 100 Hz the arc would occasionally lock on to the interelectrode axis for a brief moment and then flip back to the unstable state as before. The arc stabilization is not a continuous process as one might expect, but instead the arc would randomly break in or out of the stabilized condition. By the time the repetition rate was increased to 150 Hz and beyond the arc remained stable practically 100% of the time. The reason for the two discrete states of arc stability is not fully understood at the present time, but might have something to do with the establishment of a steady state operating condition with the vortex and the production of hot gases and residual ions.

3.4 Conclusions

It has yet to be demonstrated that the unconfined vortex flashlamp will stabilize a high energy discharge at gas flow rates as large as that used for the present flashlamp. However, from vortex pressure measurements previously made there is no reason to believe that the arc cannot be stabilized at high enough gas flows, the estimate being 7 ℓ/s for the required flow. This removes one of the advantages hoped for in the unconfined vortex design, however.

It was demonstrated that high energy discharges could be stabilized at flow rates as low as a few tenths ℓ/s with a dc sustainer operating between the electrodes. The sustainer stabilization was good only for repetition lower than 2 Hz. For higher repetition rates the sustainer did not have time to reestablish itself. This condition might be improved with larger gas flows. The most interesting results were obtained when 2J arc discharges were run at repetition rates greater than 150 Hz with an external spark gap. In this case the arc self stabilized even though the gas flow was quite small.

In conclusion, then, if one wishes to opt for a large single pulse energy at lower repetition rates (e.g. 500 to 1000 J input at 10 to 20 Hz) to reach a specified average laser output with the present size geometry, the unconfined vortex design has good promise. To use this design the spherical laser pumping cavity would have to be ruggedized to withstand the large shock waves generated by the discharging arc. In addition, the gas flow requirements may be higher than in the present system. A principal advantage of the high single pulse energy, low repetition rate operation would be the elimination of the dye change over problem one has at the higher repetion rates.

REFERENCES

III.1 UARL Technical Proposal P-M355 November 1973.

III.2 UARL Semi-Annual Technical Report 1/1/73 - 6/30/73 M921617-2 "High Power Dye Lasers".

SECTION IV

Optical Spectral Measurements On An Unconfined Arc Discharge

4.1 Introduction

There have been several reports made in the recent literature (Ref. IV-3) of flashlamp pumped dye lasers whose electrical input to laser output efficiency is 2 to 4 times larger than what we observe with our vortex lamp system and what many others have observed with their conventional flashlamp dye lasers. Since the pumping geometry and dye solutions have been fairly well characterized, a most likely place to look for an improvement in efficiency in our system is with the arc discharge. The optical radiation from the vortex stabilized arc that uses an argon, CO_2 gas mixture has been analyzed in part by M. E. Mack (Ref. IV-4). In particular Mack measured a 13% efficiency for electrical input to optical output. In addition, measurements have been made in a test lamp comparing argon and xenon with additive gases by measuring the fluorescence output of an irradiated dye solution (Ref. IV-5).

In order to gain a better understanding of the radiation properties of the unconfined arc, however, and how these properties depend on gas composition and electrical parameters, we built a pulsed arc lamp that could be evacuated and filled with different constituent gases. Absolute spectral irradiance data is then taken for different gases and gas compositions with a calibrated spectro-radiometer. In the next few sections we will describe the arc lamp used for the measurements and the calibration of the spectrometer and detector used for the irradiance measurements. We will then describe the initial measurements made with the system, discuss some of the problems encountered, and then define future measurements to be made with the system.

4.2 Experimental Set-Up

A 6 cm cap, arc discharge lamp was constructed from a 6 inch high by 4 inch id heavy wall pyrex tube and sealed with aluminum end caps to which electrodes were attached. A two inch id pyrex tube that has a demountable fused quartz window was attached to the side of the arc chamber to allow for observation of the arc light at right angles. A portable gas handling system was built to evacuate and fill the arc lamp with different gases. The top and bottom end plates to which the electrodes are attached are connected by a strip line to a 2 μf/25kV low inductance capacitor. The capacitor is discharged in the arc lamp by a third electrode trigger that runs coaxially down the center of the upper arc electrode. A Rogovski coil is placed around the return lead to the capacitor to monitor the current. The discharging arc is far enough from the walls of the pyrex chamber to be unrestricted, but no means has been provided for arc stabilization. The arc lamp was then placed 2.26 meters away from a diffuse

reflecting screen that was coated with Eastman high reflectance paint. Black velvet cloth was placed between the lamp and screen to prevent reflected light from illuminating the screen. In addition, a large stop with a slit aperture was placed in front of the lamp so that only a 2.65 mm segment of the arc would uniformly irradiate the screen.

A Jarrell Ash $\frac{1}{4}$ meter monochromator was then placed 72 cm from the screen at an angle of 12^{o} to the centerline between the arc and screen so as not to block the illumination from the arc. The input of the monochromator, therefore, intercepted a fixed solid angle of light from the screen. A photomultiplier detector that is sensitive from 200 to 700 nm, was placed at the output of the monochromator. Using a standard lamp to illuminate the screen at a known distance, the monochromator and detector response could be calibrated for a known spectral irradiance in watts/cm^2-nm on the screen. It is important to take irradiance measurements from a screen rather than direct radiance measurements from the lamp in order to illuminate the monochromator's grating and detector's photocathode in the same manner with both the standard lamp and the arc lamp. In particular, it was found by sweeping a He-Ne laser spot around on the screen that the monochromator and photodetector is indeed sensitive to the direction of a localized collection of light. A 200 watt iodine quartz lamp with a regulated power supply and high accuracy ammeter was used to calibrate the system (Ref. IV-6). The calibration accuracy was estimated to be 12% (Ref. IV-7). For light attenuation and spectral blocking that was required at certain wavelengths 4 neutral density and 6 color filters were calibrated throughout the spectrum. A calibration between 150 μm and 25 μm monochromator slits was also made to allow for a higher degree of attenuation when using the arc lamp.

4.3 Effects of Additive Gases

Current measurements taken when the capacitor is discharged into the arc lamp show an underdamped circuit that rings for 5 periods. The time for the first period was 4.3 μs and each successive period becomes slightly shorter since the arc acts as a non linear circuit element. The total circuit inductance of the arc lamp, as determined from the ringing frequency, is 227 nh. The vortex stabilized lamp, on the other hand, has an inductance of 155 nh and correspondingly is much better damped. Besides arc stabiliation, the discharge dampening represents a major difference between the two lamps so that conclusions drawn from the measurements on the unstabilized arc lamp may not, exactly carry over to the vortex lamp.

If the arc lamp is filled with 1 atm. of pure argon after filling and flushing several times it will self discharge at around 9kV or 81 J discharge energy. On the other hand, if 50 to 100 m. torr of residual gases like air or N_2 is left in the lamp before filling with argon the self breakdown voltage will be increased

to 16 kV. This allows us to trigger the discharge with the third electrode for lower voltages. All of the measurements reported here were taken at 14.2kV which corresponds to 202 J discharge energy. It was noticed that the output from the arc lamp with one atmosphere of argon was sensitive to the amount of the residual gases. Figure IV-1 shows a plot of the time integrated light output at 270 nm on a relative scale vs the partial pressures of CO_2 and SF_6 in 1 atmosphere of argon. With more than 6 torr partial pressure of CO_2 the lamp became very difficult to trigger. Triggering difficulty arose after about 200 m torr of SF_6 due to the high breakdown strength of this gas. With nitrogen, which has a lower hold off voltage than SF_6 but about the same as CO_2, we could add up to 70 torr as shown in Fig. IV-3 and still trigger the discharge. The results shown in Figs. IV 1-3 demonstrate the importance of the additive gas not just to give better voltage hold off characteristics but also to improve the light output from the lamp. A factor of 2 in light output is clearly seen from these results. Figure IV-2 shows results similar to Fig. IV-1 for CO_2 except the observation wavelength is 500 nm. The increase in the light output with the additive gases, therefore, is probably spectrum wide. The mechanism producing the increase in light output with the additive gases is not understood at the present. Additional research along this avenue could lead to more improvements in the overall lamp output.

4.4 Spectral Measurements

The photomultiplier detector used to measure the spectral irradiances was current limited at about 0.15 mA. This means that we are limited to the detection of low light levels in pulsed operation at the rate of about 10^3 detected photons per μsec. As a consequence, we had to attenuate the reflected arc light from the screen at the input to the monochromator by factors ranging from 30 to 100. The current output from the photomultiplier is integrated to produce a voltage signal on a capacitor. The peak voltage, which can be related to the total charge generated by the photomultiplier, is then sampled by a sample-hold circuit that is synchronized with the discharge pulse. The capacitor voltage is then read by a digital voltmeter.

The arc lamp output was found to fluctuate with a standard deviation of 10.2% about an average value for a given discharge energy and wavelength. Standard deviations no greater than 2% could be expected from the signal statistics. A multiple exposure photo of the discharge current scope traces indicated that the current is consistent from shot to shot; but a multiple exposure photo from a photodiode that could monitor the time response of the arc lamp light indicated that the fluctuations were prinicpally due to the generated light output. This could possibly be due to the fact that the arc is not stabilized and has a slightly different path length for each discharge.

INTEGRATED LIGHT OUTPUT FROM ARC LAMP

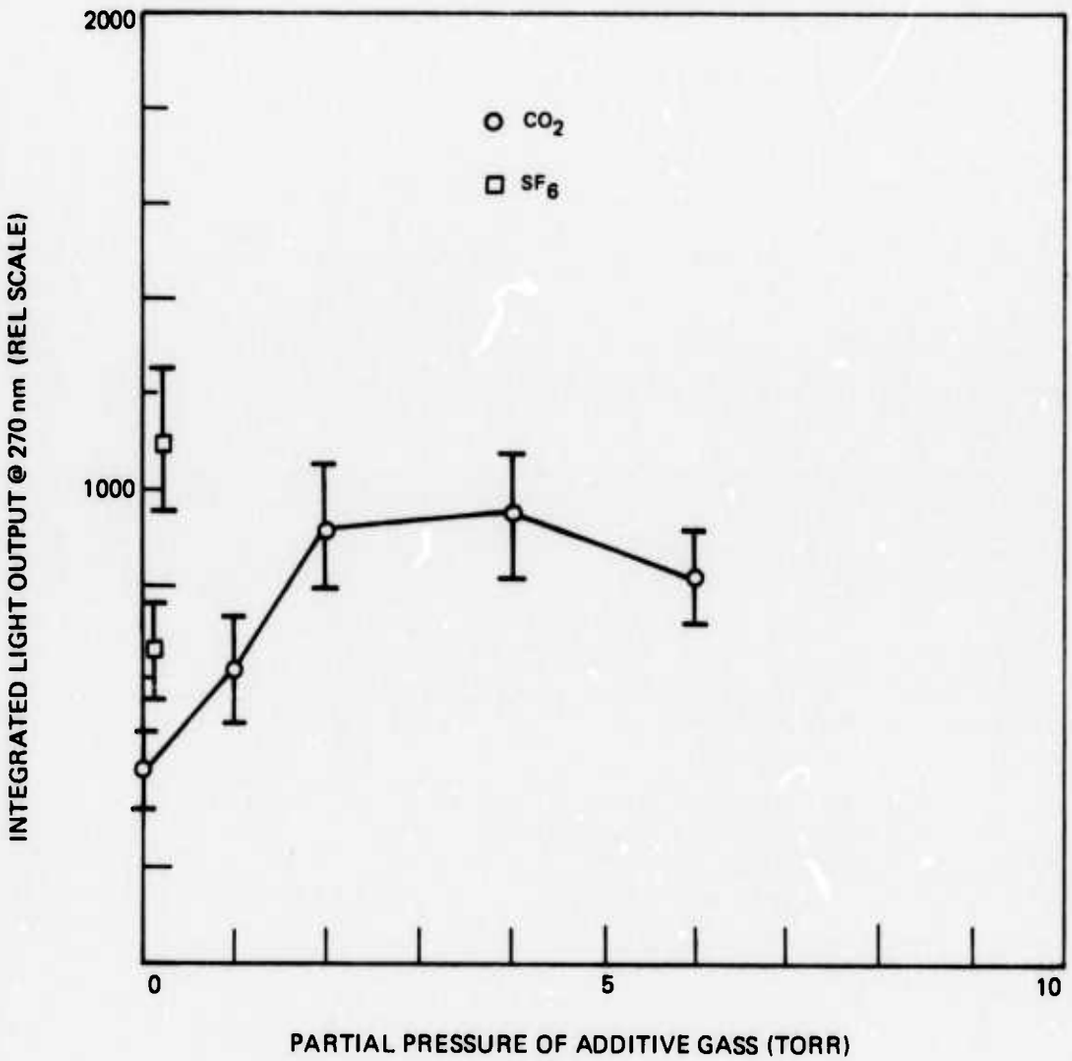

FIG. IV-2

INTEGRATED LIGHT OUTPUT FROM ARC LAMP

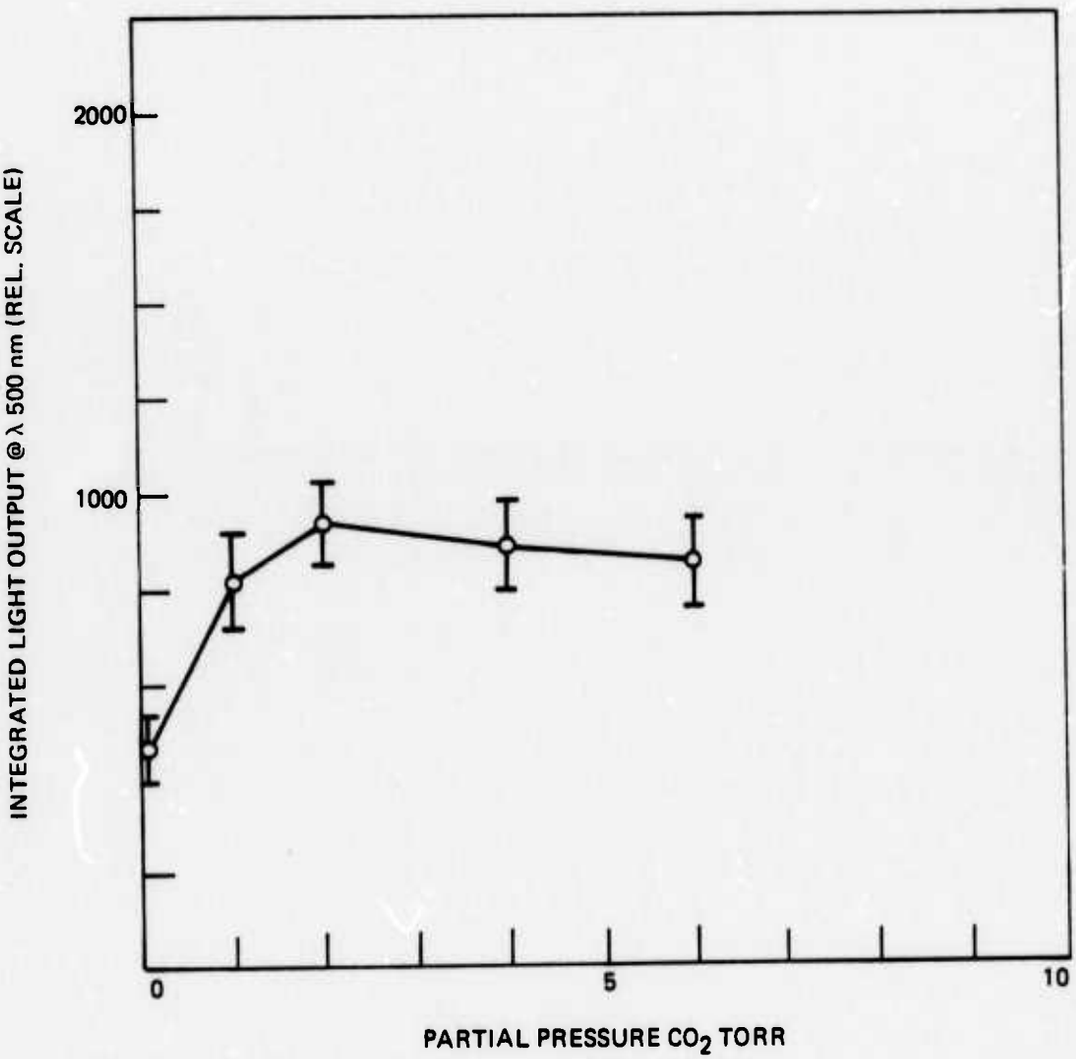

N02-195-9

N921617–5

FIG. IV-3

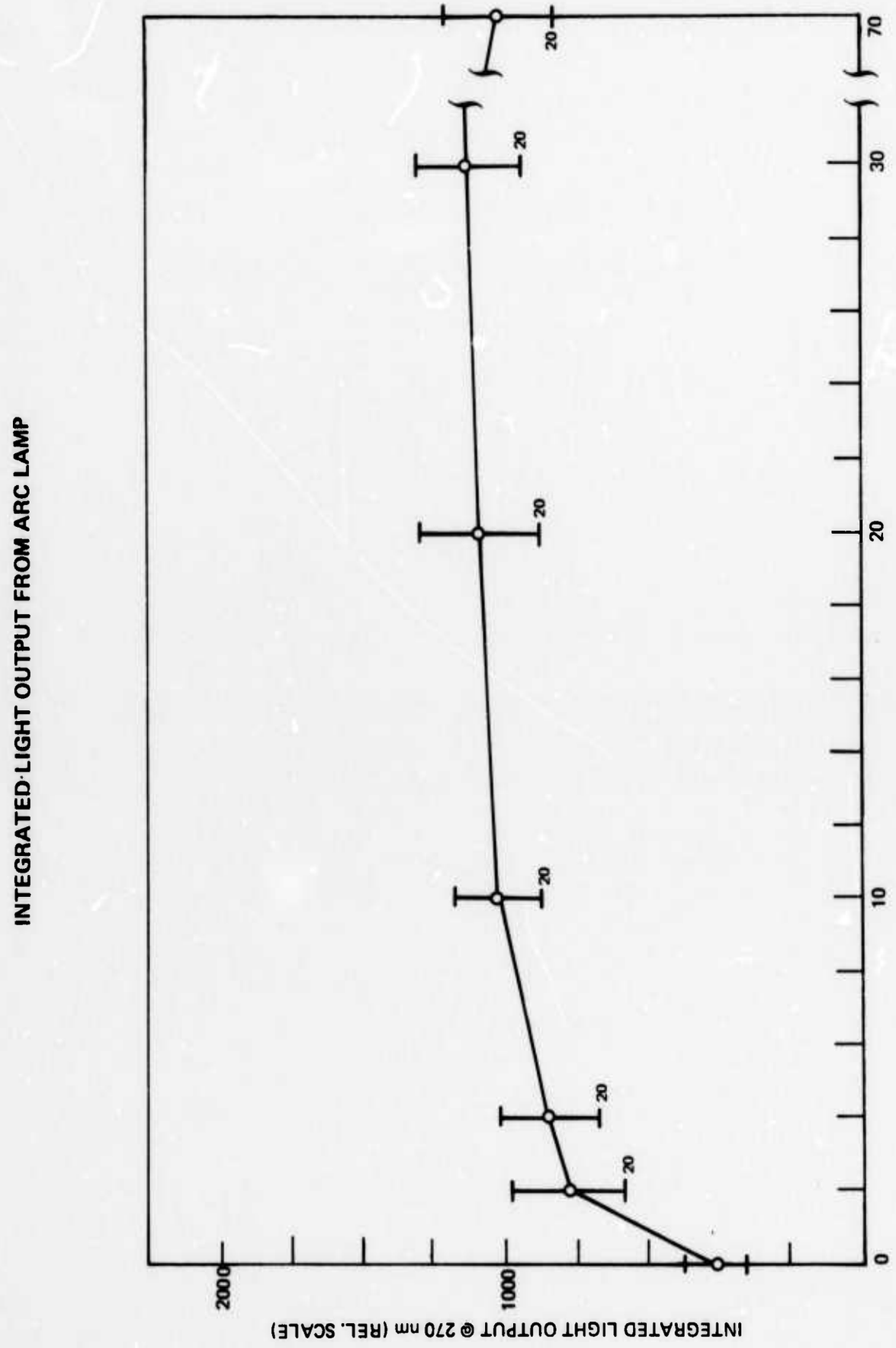

N02–195–11

To obtain a data point at each wavelength ten shots were averaged together. Figure IV-4 shows the results of measurements of the time integrated irradiance on the screen from the arc lamp in nJ/cm^2-nm. From these results we see that the time integrated output from xenon in the unconfined arc is larger than that for argon. This is particularly true in the uv where the output is three times as great. In the wavelength interval of 450 nm to 550 nm, which corresponds to the principle rhodamine 6G pump band, xenon emits about 74% more light energy. There is a catch to this output, however, as we can see from Fig. IV-5 which shows the time response of the 200J pulses in xenon and argon as taken with a photodiode with an S-5 wavelength response. The peak height of the xenon pulse given on the first current swing is only about 30% higher than the peak height of the argon pulse. The peak intensity of the xenon is considerably less than one would expect for the uv and visable responding photodiode based on the integrated output. It is noticed, however, that the xenon puts out considerably more light intensity in the succeeding current swings of the under damped discharge and consequently more light energy.

The area under the argon curve in Fig. IV-4 represents the energy emitted by 0.265 cm of the arc in a solid angle of $1/R^2$ where R is the distance from the arc to the screen. Since the arc can be approximated as a lineal source at the distances used, we can estimate the total light energy emitted by the arc by multiplying the area under the argon curve in Fig. IV-4 by the ratio of the total solid angle of a Lambertion emitting lineal element (π^2) to the solid angle from the arc to 1 cm_2 on the screen ($1/R^2$) and the ratio of the length of the arc (6 cm) to the aperture height (265 cm). This gives 26.3 J for 202 J electrical input or an efficiency of 13%. This agrees with Mack's calorimetric measurements in Ref. IV-4.

Using the average time of the pulses from Fig. IV-5 we can determine the spectral irradiance (H_λ) of the arc lamp on the screen in $Watts/cm^2$-nm. With this data we can then determine the spectral radiant intensity per unit length for the arc (J_λ) in Watts/ster-nm-cm by dividing H_λ by the solid angle from the arc to 1 cm^2 on the screen and by the aperture height. Figure IV-6 shows the peak spectral radiant intensity of xenon and argon. Only for wavelengths shorter than 320 nm is xenon significantly more intense than argon. The broken line in Fig. IV-6 shows for comparison the spectral radiant intensity of a 25,000°K blackbody that has a diameter of 0.7 cm. This diameter corresponds to the arc diameter as estimated from photographs. One can see that the arc becomes optically thin for wavelengths in the near uv and approaches a blackbody only in the red and infrared.

Figure IV-7 shows a plot of the light output energy of the arc at λ500nm vs the discharge energy for both xenon and argon. As one would expect the output is proportional to the input energy. In Fig. IV-8 we have plotted the light output

TIME INTEGRATED SPECTRAL IRRADIANCE OF ARC LAMP

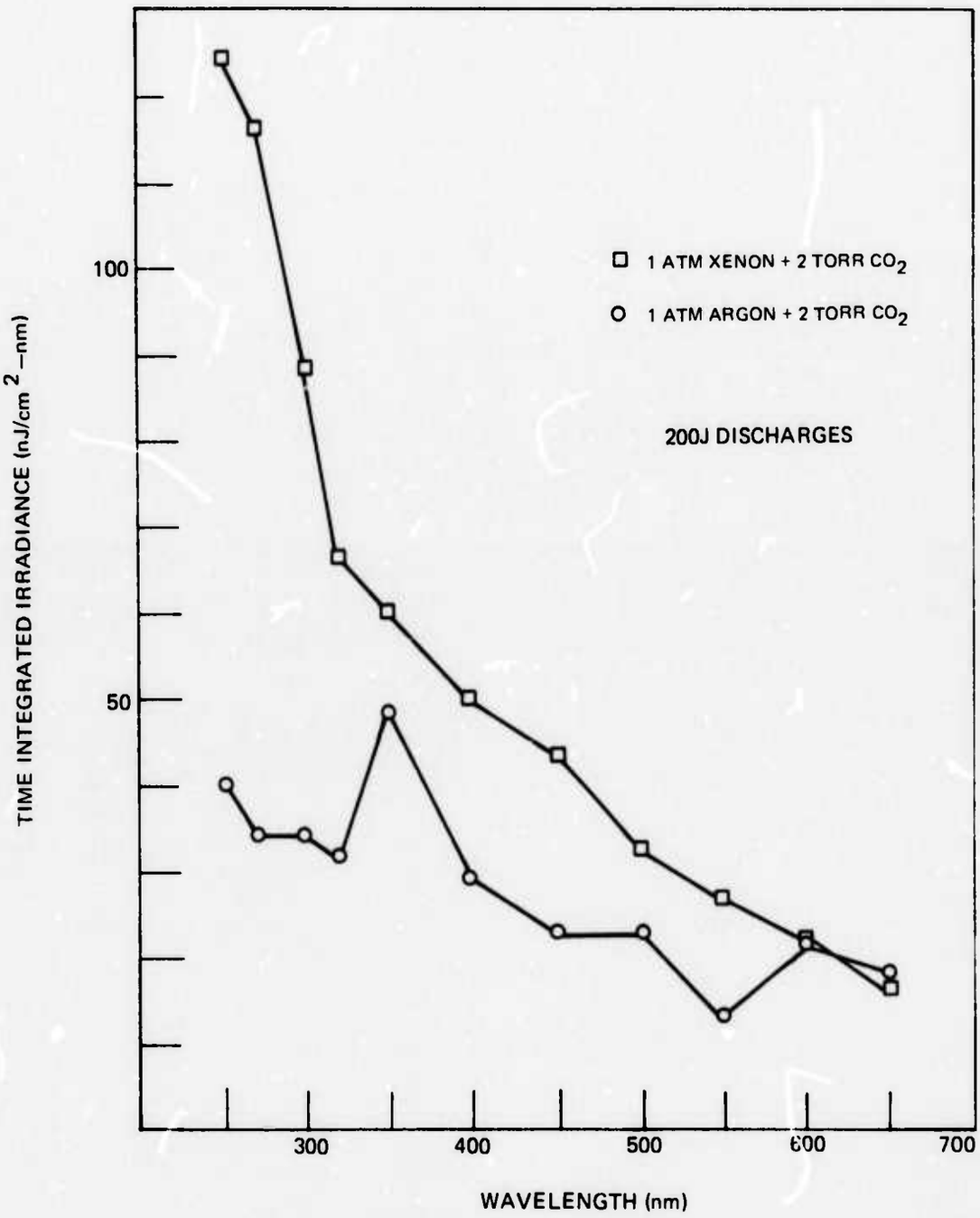

N02-195-16

TIME RESPONSE OF LIGHT OUTPUT FROM ARC LAMP

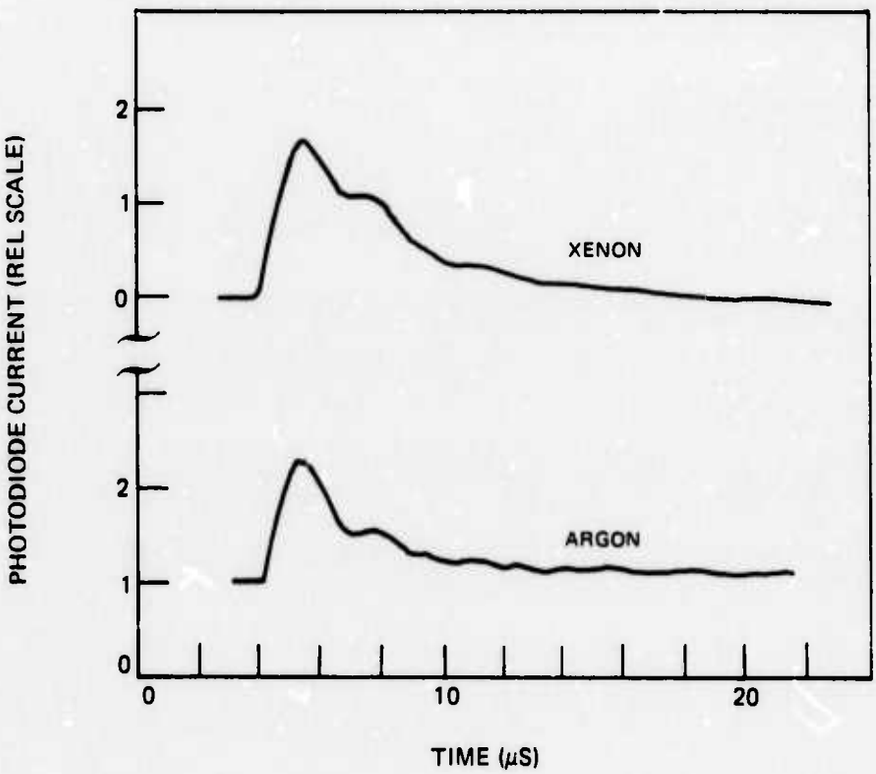

N02-195-14

FIG. IV–6

SPECTRAL RADIANT INTENSITY OF ARC LAMP

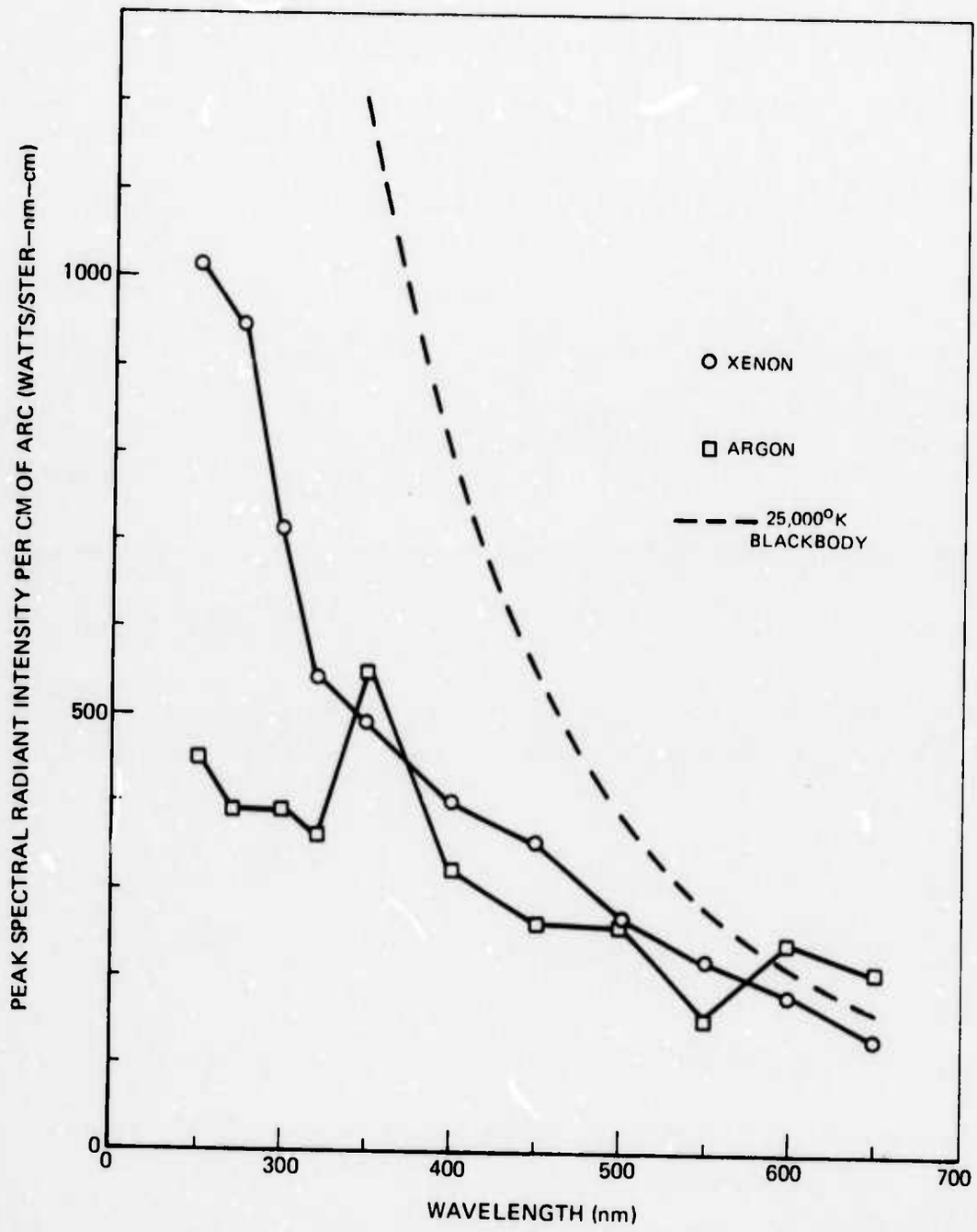

N03–11–1

FIG. IV-7

LIGHT OUTPUT OF ARC LAMP VS DISCHARGE ENERGY

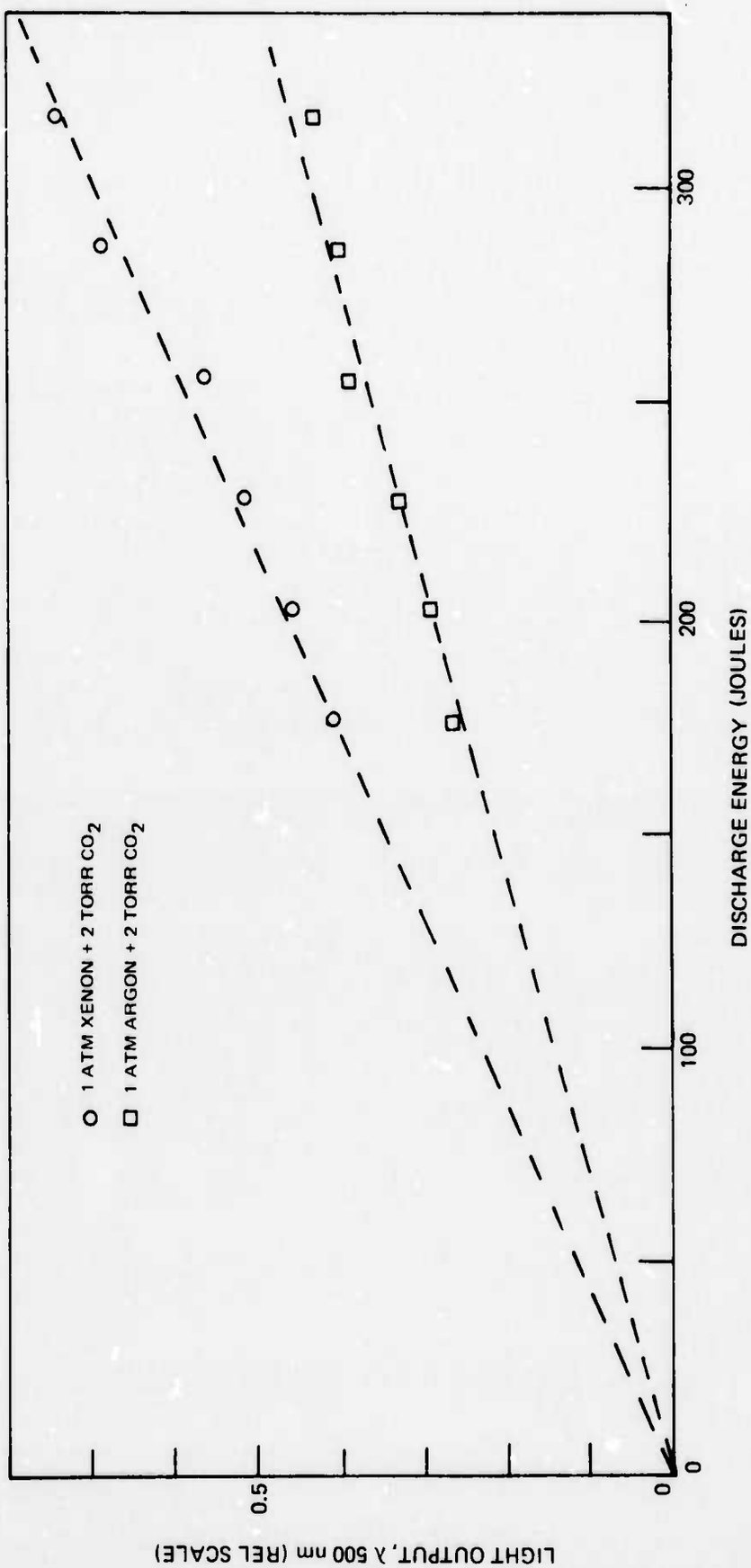

N02-195-12

FIG. IV-8

LIGHT OUTPUT OF ARC LAMP VS GAS PRESSURE

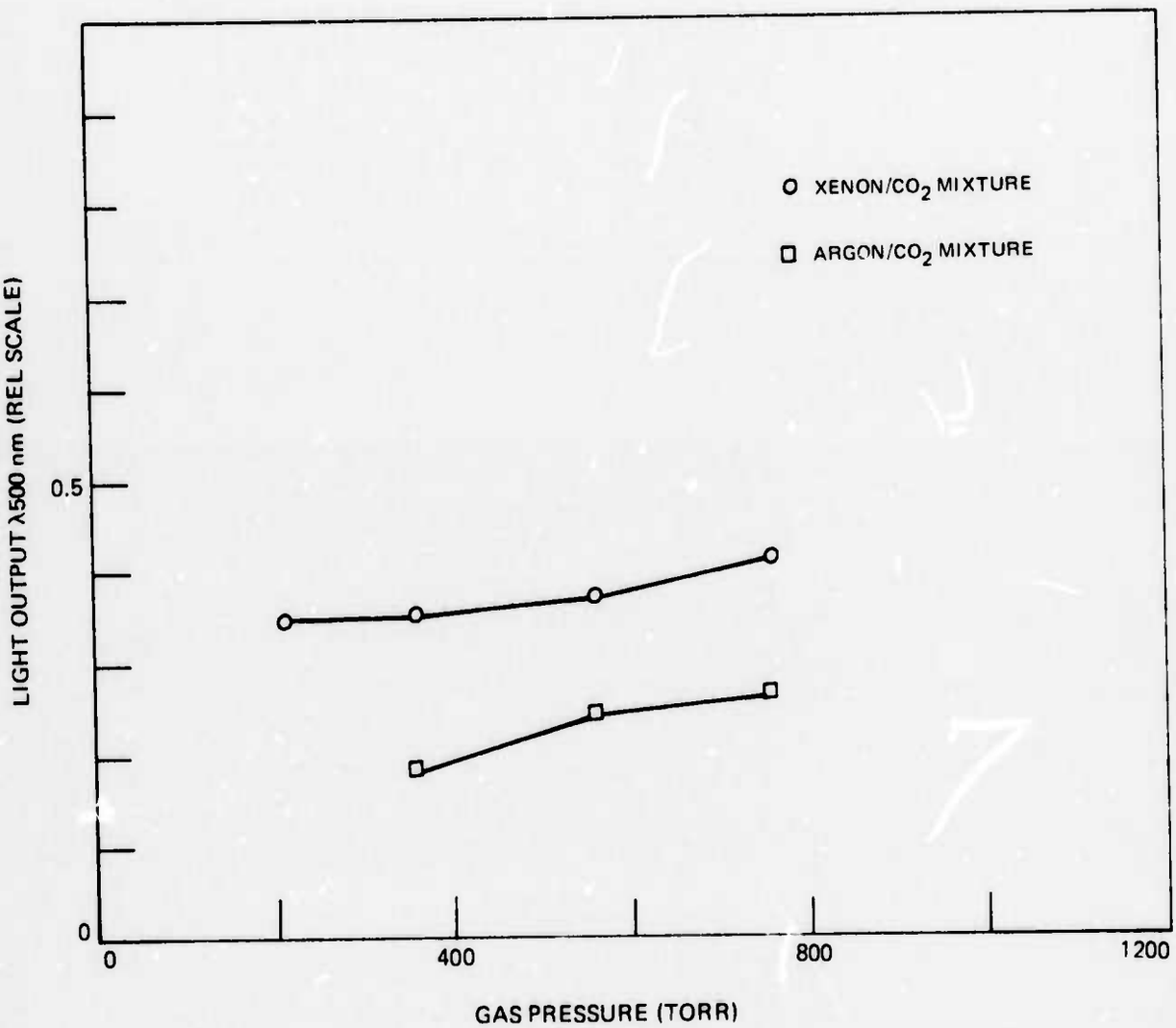

N02-195-13

energy vs the arc lamp pressure at constant rare gas to CO_2 ratio. Recent measurements on argon at pressures down to 15 torr indicate a steady fall off of light output with decreasing pressure. This leads one to believe that some of the low pressure, wall stabilized xenon lamps reported in the literature (Ref. IV-2) are really ablating wall lamps with the ablation products contributing heavily to the spectral output and the higher efficiencies.

4.5 Conclusions

The spectral data comparing argon to xenon corroborates previous results on the fluorescence measurements (Ref. IV-5); namely, that while xenon gives a larger light energy output its peak output power in the near uv and visable is not significantly greater than that of argon. Most of the increased light output comes from more light generated in the second and third current reversals of the underdamped discharge. As applied to the vortex lamp system this means that we could extend the pumping pulse width by using xenon but could not obtain a very large increase in the peak pumping power at the visable and near uv wavelengths. If the dye lasing does not terminate early from lack of triplet quenching or from thermo-optic distortion then one could expect an increase of about 30 to 50% in laser energy output from using xenon instead of argon.

Another interesting observation was the dependence of the lamp output on the amount and type of additive gases mixed with the argon. Anliker et al. (Ref. IV-1), who obtained 1.2% laser efficiency, used ablating wall lamps that do not have a well characterized gas composition; and Dzyubenko et al. (Ref. IV-2), who obtained a 0.75% laser efficiency, used a low pressure (15 torr), wall stabilized xenon lamp that undoubtedly must have had a considerable amount of ablating wall products in the arc as indicated by the reduced light output we observe with decreasing pressure. The amount and type of ablation products may be very significant in the light generation efficiencies. The measurement of the light generating capabilities with more and different gas species is an important area for future work. In a review article Marshak (Ref. IV-8) also presented some experimental data on bounded arc, pulsed discharges that demonstrates enhanced output intensity with mixtures of 66% xenon and 26% N_2. Marshak's data also demonstrates the saturation in the intensity of the arc with larger input power. In addition to examining other additive gases, a hole could be drilled in the lower electrode for placement of substances that could be vaporized into the arc.

At present the effectiveness of the uv light in pumping the rhodamine 6G dye solutions as compared with the visable light is not clearly defined. The lamp filtering experiments described in section V of this report indicate the dyes uv pump band is not nearly as effective as the visable pump band. An important test that we hope to perform is to determine the fluorescence efficiency of the dye for various input wavelengths out to 250 nm. This would permit us to take a known or measured flashlamp spectrum and pulse shape to apply to a laser computer program now being developed for dye laser output power.

REFERENCES

IV-1. P. Anliker, M. Gassmann, and H. Weber "12 Joules Rhodamine 6G Laser" Opt. Comm. 5, 137 (1972).

IV-2. M. I. Dzyubenko, I. G. Naumenko, V. P. Pelipenko and S. E. Soldatenko "High Efficiency Visible-Band Laser Using Dyes." ZhETF Pis. Red. 18, 43 (1973).

IV-3. H. W. Furumoto and H. L. Ceccon, "Optical Pumps for Organic Dye Lasers" Appl. Opt. 8, 1613 (1969).

IV-4. M. E. Mack, "Vortex Stabilized Flashlamps for Dye Laser Pumping" Appl. Opt. 13, 46 (1974).

IV-5. "Proposed Further Development of High Power Dye Laser Technology" UARL Proposal P-M355 November 1973.

IV-6. R. Stair, W. E. Schneider, J. K. Jackson "A New Standard of Spectral Irradiance" Appl. Opt. 2, 1151 (1963).

IV-7. Private Communication with The Eppley Laboratory, 12 Sheffield Ave., Newport, R. I.

IV-8. I. S. Marshak "Strong Current Pulse (Spark) Discharges in Gas, Used In Pulsed Light Sources" Sov. Phys. Uspekli 5, 478 (1962), Ups. Fig. Nauk, 77, 229 (1962).

SECTION V

PASSIVE FILTERING

5.1 Experiment and Results

The importance of reducing triplet state populations in laser dyes is well known (Ref. V-1). Oxygen is one of the most effective triplet state quenchers for Rhodamine 6G but tests in the vortex flashlamp dye laser confirm the generally held view that it also drastically reduces the lifetime of the dye. Chemical triplet quenchers have been reported, however, that are almost as effective as oxygen (Ref. V-2). In addition the number of photobleached molecules generated by flashlamp pumping of Rh 6G in methanol is about four times lower with the triplet state quencher C_8H_8 than with oxygen (Ref. V-3). These results are further evidence of the lifetime degrading effects of oxygen.

C_8H_8 has been tested previously with Rhodamine 6G-ethanol in the vortex flashlamp dye laser with little success. Recent results in the literature (Ref. V-4), however, indicate that substantial increases in efficiency can be obtained even at high pump energies. Previous tests of the laser have also indicated that the laser pulse is terminated by thermal effects primarily. Thus, the use of a triplet quencher could be of little value.

Heating of the dye is the result of radiationless transitions from the second excited singlet state S_2 to the first excited singlet state S_1, from S_1 to the triplet state T_1, and a host of other transitions resulting from absorption of the fluorescence by the population of T_1 and subsequent relaxation of these excited states. The most efficient pump wavelength would be the peak of the primary absorption band at 530nm. Because of the high effective color temperature of the lamp, most of the fluorescence is a result of the UV absorption bands which peak at 350nm, 275nm, and 250nm, and others extending to below 200nm. These considerations raise the possibility of simultaneously decreasing the thermal problem and increasing the efficiency.

Tests were made of the efficiency of a methanol solution of Rhodamine 6G with C_8H_8 added. The dye cell was a double wall arrangement consisting of an 8 x 10 mm inner tube containing the dye and an outer tube 13 x 15 mm coaxial with the smaller tube. Suitable connections are made so that a liquid filter may be flowed in the space between the two tubes. For the experiments described below the tubes were commercial grade fused quartz.

The solution was 4×10^{-4} molar Rhodamine 6G and 2×10^{-3} molar C_8H_8 in UV grade methanol. Ordinary Kodak Rhodamine 6G chloride was used. Using the standard 2μf capacitor to drive the lamp tests were made using various organic solvents in

the dye cell jacket to vary the cutoff wavelength of the pump radiation. The mirror reflectivity was simultaneously optimized. During the lamp pulse the dye was not flowing but was allowed to come to thermal equilibrium as judged from the appearance of a He-Ne probe beam passing through the cell and reflected from the 100% mirror.

Filter solvents used and their cutoff wavelengths were: methanol, 200nm; carbon tetrachloride, 260nm; orthodichlorobenzene, 295nm. These solvents selectively block light from the bands below 200nm, the 250nm band, and the 275nm bands respectively. At 100 joules input energy to the vortex lamp the pulse energies for various cutoff wavelengths were: 200nm - 300 millijoule, 260nm - 360 millijoule, 295nm - 300 millijoule. A typical output energy for the optimum de-gassed ethanol solution of Rhodamine 6G would be 250 millijoules. The 0.36% efficiency obtained is the highest ever obtained from this laser. Higher efficiencies may be obtainable from Rhodamine 6G tetrafluoroborate - C_8H_8 solutions.

At 225 joules input energy to the flashlamp, maximum laser energy was 650 millijoules obtained with a 30% mirror and the 260nm filter. The output with the 295nm filter was slightly lower and with the 200nm filter was 75% lower than with the 260nm cutoff. This may be compared with results obtained in a related contract effort where 720 millijoules was obtained at 225 joules input from an oxygen saturated Rhodamine 6G tetrafluoroborate-ethanol solution.

Figure VI-1 shows the changes in shape of the laser pulse resulting from addition of C_8H_8 and with changes in the cutoff wavelength. The pulse is clearly lengthened with addition of the triplet state quencher and optimization of the filter cutoff. In this connection it may be mentioned that a 2×10^{-3} molar solution of C_8H_8 in UV methanol is transparent throughout the visible and cuts off at 200nm.

In order to test the possibility for obtaining longer pulses a pulse forming network was made by adding a 3.6 μf capacitor in series with a small inductance to the 2 μf capacitor normally used (in parallel). A small resistance was included in series with the inductor to prevent ringing and possible damage to the small 3.6 μf capacitor. Figure V -2 show the resulting output intensity of the vortex flashlamp with a 10 KV charging voltage. This amounts to a calculated maximum input energy to the lamp of 280 joules. The laser output energy was 420 millijoules. It is seen that lasing is possible over extended pulses up to 5 μsec. though with reduced energy in the tail. This is the longest laser pulse ever obtained with this laser.

Tests using a Pyrex cell (cutoff about 300nm) 15 x 13 mm were made but were inconclusive because the concentration and cell size were not optimized. Using the same solution as for the tests above, maximum output energy at an input energy of 225 joules was 350 millijoules using a 50% mirror.

FIG. V-1

LASER PULSE WITH TRIPLET STATE QUENCHER

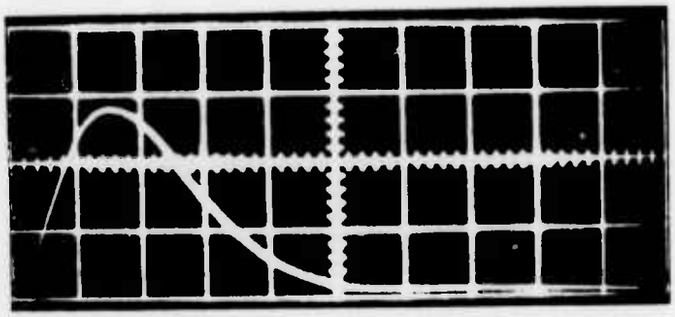

(a) LASER PULSE (TYPICAL), RHODAMINE 6G IN DE–OXYGENATED ETHANOL, 100 Joule INPUT, 1/2 μsec/div

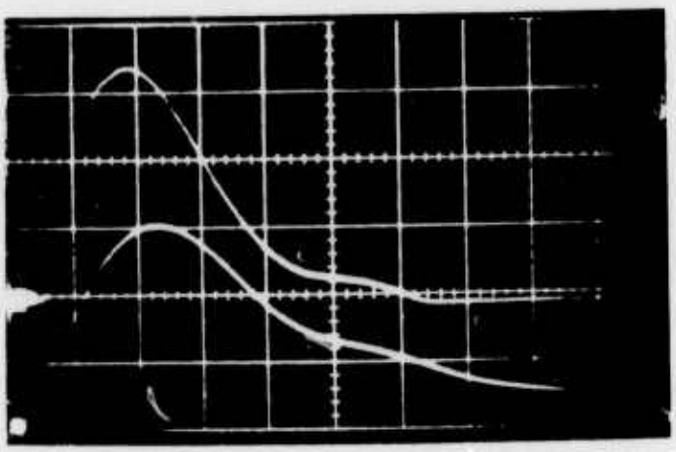

(b) UPPER TRACE: LASER PULSE, Rh6G + COT, 200 nm CUTOFF FILTER LOWER TRACE: FLASHLAMP INTENSITY, 100J, 1/2 μsec/div

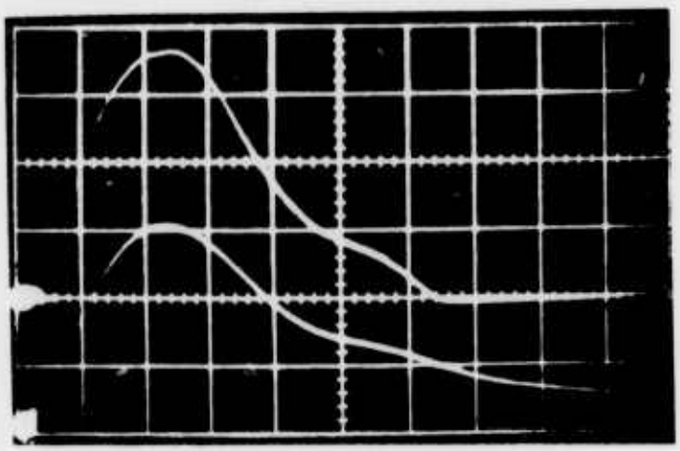

(c) UPPER TRACE: LASER PULSE Rh6G + COT, 260 nm CUTOFF FILTER LOWER TRACE: FLASHLAMP INTENSITY, 100 J, 1/2 μsec

FIG. V-2

EXTENDED PULSE LASER

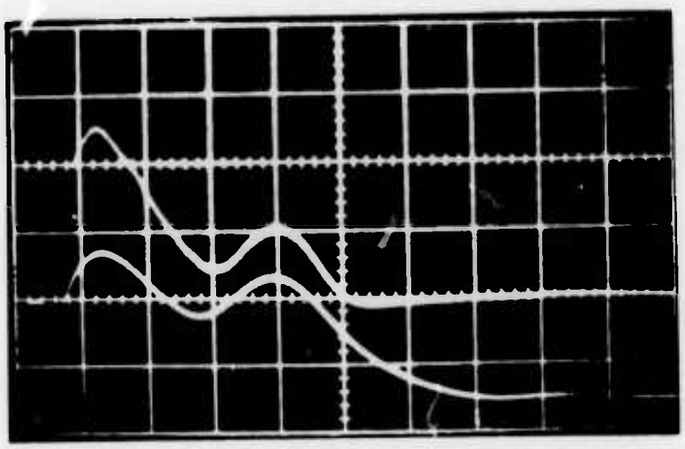

UPPER TRACE: LASER PULSE, 1 μsec/div,
TOTAL ENERGY ~460 Millijoule

LOWER TRACE: FLASHLAMP PULSE, INPUT ENERGY 280 Joule

5.2 Discussion

The foregoing experiments indicate the importance of the inter-relationship between the flashlamp pump spectra and the dye solution. Low quantum efficiency pump radiation not only enhances the thermal cutoff problem but also may interfere with the action of triplet state quenchers. In these experiments it appears that blocking UV radiation lying outside of the absorption band of the C_8H_8 is necessary to get quenching of the triplet state.

The exact role of the filter in increasing the efficiency of the dye has not, of course, been established. Experiments have not been made, for example, to determine if the efficiency of Rhodamine 6G can be increased by filtering the pump light. These and other experiments would be necessary to determine whether the filtering merely leads to increased dye quantum efficiency for the particular solvent, decreases the thermal cutoff problem in this laser, interferes with the effectiveness of the triplet quencher in de-activating the triplet state, or perhaps causes the generation of states in the C_8H_8 molecule which absorb the dye fluorescence. Because of the complexity of the problem and lack of knowledge of details of the interaction of this dye with C_8H_8 the problem will require largely an experimental attack.

The particular use of flowing solvents in a jacket surrounding the dye cell has several advantages. Since the filter is absorptive the use of a flowing medium allows external cooling to remove absorbed heat. In addition the filter may be cooled or heated if desired in order to create temperature gradients for compensation of thermal lensing in the dye. It may also be desirable to operate the dye at reduced temperatures in order to achieve more favorable values of the change of index of refraction with temperature and so reduce thermal distortion.

As is indicated in a following section, increased optical efficiency of the flashlamp is obtained in various gas mixtures as the result of a longer and broader light pulse. If the laser pulse is cut off by thermal distortion or triplet states, however, the additional light in the tail of the lamp pulse cannot be utilized. The long pulse experiment described here shows that longer output pulses can be generated in the present laser. The lower efficiency in the tail might possibly be increased through better matching of the pump spectrum to the dye. Longer pulses may also be required for some system applications. The experiments show operation for the first time of the vortex lamp with longer pulses. It should be possible to increase the pulse length without limit in this lamp, thus raising the possibility of CW laser operation if high enough pump intensities could be achieved.

The foregoing raises the question of short versus long pulses in increasing the efficiency of the laser and generating maximum power. Assuming a time independent lamp spectra efficiency is enhanced by very short pulses because triplet state losses

are avoided and thermal cutoff occurs after the end of the lamp pulse. In this case, lamp pulse energy is limited by pulse length and high average power operation requires very high repetition rates with the attendant problems of lamp circuitry and high dye cell flow rates. Relatively long (greater than about 5 μsec.) pulses are limited by the extent to which problems of triplet state quenching and thermal cutoff can be avoided. The present state of the art appears to be near 5 μsec. for high energy dye lasers. For the present lamp using a single storage capacitor and assuming critical damping, increases in input energy will result in higher color temperatures and less efficient pumping of the dye. These considerations further indicate the importance of determining the temporal evolution of the flashlamp spectrum for various gas fill mixtures and of optimizing dye solution, dye cell and mirror reflectivity with lamp spectrum.

5.3 Summary

Experiments with passive filtering of the pump radiation show that it can be used to achieve higher efficiency. The 0.36% efficiency achieved was the highest so far for this laser. Further increases up to 1% might be possible with an optimized pump source. Work with highly pure dyes on an associated contract has shown that up to 720 millijoules per pulse can be achieved with this type of laser. Long pulse operation of the laser was demonstrated for the first time with lengths of up to 5 μsec. This shows that some freedom in optimizing flashlamp pulse energy versus pulse width is available.

In future work we plan to study the use of other triplet state quenchers and solvents with Rhodamine 6G, particularly water because of its desirable thermal properties. Efficient excitation transfer in Cresyl Violet-Rhodamine 6G mixtures has recently been reported (Ref. V-5). Although an extensive search has not been made it appears that Brilliant Sulphaflavine (lasing from 508nm to 574nm) (Ref. V-2) or Coumarin 6 or Coumarin 7 (Ref. V-6) might be useful for pumping Rhodamine 6G in mixtures. The use of the passive filtering arrangement permits limited exploration of the effect of flashlamp spectrum on the efficiency of these and other dye solutions. Measurements of the flashlamp spectra should also permit some analytical modeling of the pumping of the various dyes.

REFERENCES FOR SECTION VI

V-1. Marling, J. B., D. W. Gregg, and S. J. Thomas: IEEE J. of Quantum Electronics QE-6, 570 (1970).

V-2. Marling, J. B., D. W. Gregg, and L. Wood: Applied Physics Letters 17, 527 (1970).

V-3. Weber, J.: Optics Communications 7, 420 (1973).

V-4. Anliker, P., M. Gaussmann, and H. Weber: Optics Communications 5, 137 (1972).

V-5. Dienes, A. and M. Madden: J. Appl. Phys. 44, 4161 (1973).

V-6. Tuccio, S. A., K. H. Drexhage, and G. A. Reynolds: Optics Communications 7, 248 (1973).